

Axisymmetric Tokamak Equilibria computed with a Predefined Safety Factor Profile as CHEASE input

Lily Blondel, O. Sauter and A. Merle

Ecole Polytechnique Fédérale de Lausanne (EPFL), Swiss Plasma Center (SPC),
CH-1015 Lausanne, Switzerland

Lausanne report LRP 07/2016
July 2016

Contents

1	Introduction	3
2	Tokamak equilibria	4
2.1	The Grad-Shafranov Equation	4
2.2	CHEASE parameters	5
2.2.1	Definition of the safety factor q	5
2.2.2	Definition of the toroidal current density j_ϕ and its surface average I^*	5
3	Using a predefined q profile as CHEASE input with an external loop to find the appropriate I^* and TT' expressions	6
3.1	I^* as the surface average of the current density j_ϕ	7
3.1.1	Combining <i>old</i> and <i>new</i> I^* expressions	9
3.1.2	Using an alternative radial coordinate	9
3.2	$TT'(q)$ as input instead of $I^*(q)$	12
3.3	I^* from Antoine Merle's note	14
3.4	Testing specific q profiles	18
3.4.1	First profile	18
3.4.2	Series of four profiles	18
3.4.3	Test case with a specified profile	25
4	Implementing the procedure into CHEASE	28
4.1	Approach	28
4.2	Validation with the q profiles tested externally	33
4.2.1	First profile	34
4.2.2	Series of four profiles	34
4.2.3	Test case with a specified profile	34
5	Applying the procedure for tearing modes stability analysis	38
6	Conclusion	40
7	Acknowledgements	40
	Appendices	43
A	Selecting the updated quantity	43
B	Deriving with respect to a more stable variable	47
C	Using $TT'(I^*)$ as input	49
D	Using an alternative radial coordinate: complement	51
E	I^* from Antoine Merle's note: complement	52

1 Introduction

The CHEASE code, which has been developed at the Swiss Plasma Center, generates an accurate reconstruction of toroidal magnetohydrodynamics equilibria by numerically solving the Grad-Shafranov equation. Having demonstrated its ability to achieve good convergence while remaining fast and very flexible, this code is now extensively used at different research facilities. From two input profiles, usually the pressure and the current density as well as specified boundary conditions, the code provides a complete equilibrium description which is essential for the study of tokamak plasmas.

This project focuses on computing axisymmetric equilibria within ideal magnetohydrodynamics (MHD) by imposing a specific shape for the safety factor q . The Grad-Shafranov equation requires two free functions to be specified: one for the current density and one for the pressure ($p=nT$). Until now, the options in CHEASE allowed to give the pressure profile or its derivative on one hand and either TT' , I^* , I_{\parallel} , or J_{\parallel} on the other hand. The safety factor profile was therefore a result of the computation of the equilibrium. However, this profile and its radial derivative are essential for stability and transport issues into the tokamak. The goal of the present project is thus to modify the code so as to be able to provide a safety factor profile as a CHEASE input.

However, equilibria generated with the safety factor profile as input can easily lead to surface currents if strong variation of the derivative $\frac{dq}{d\rho}$ appears in the solution. It is therefore necessary to develop a method to avoid these problems, especially at the edge of the plasma. A further aim of this work is hence to demonstrate that there is no continuity problem within solutions computed with a q -profile as input. There are two ways of achieving this: one is to impose the current profile within one iteration to obtain the desired safety factor profile and the other is to impose the TT' profile in the same way. The two solutions are explored in this project with the purpose to determine which one is most appropriate.

Finally, the extended version of CHEASE developed in this master project is used to study the influence of safety factor profiles on the stability of tearing modes by solving the energy principle equation within the cylindrical approximation which depends directly on q , q' and q'' .

2 Tokamak equilibria

As one of Europe’s leading fusion research facilities, the Swiss Plasma Center works towards developing fusion as an energy source. Experimental research can be undertaken at the TCV (*Tokamak à Configuration Variable*) which provides unique shaping capabilities as well as a large variety of diagnostics. A wide range of research programs are run both internally and within international collaborations to try to get a better understanding of the observed physics phenomena, which is essential to provide an interpretation of the experimental results. One of these programs, the CHEASE code, which solves the Grad-Shafranov equation for toroidal MHD equilibria, was developed mainly by H.Lütjens, A.Bondeson and O.Sauter and will be used in the present work.

Being able to explore the nature of equilibria is very important in plasma physics as the plasma has to be close to an equilibrium to be confined. In this project we will focus on axisymmetric MHD equilibria and will use the cylindrical coordinate system (R, Z, ϕ) . The toroidal axisymmetry, assumed from here on, implies that all the equilibrium quantities are independent of ϕ which leads to a 2-D equilibrium.

2.1 The Grad-Shafranov Equation

The MagnetoHydroDynamics (MHD) model is a 1-fluid model extensively used in plasma physics as it can be applied in the great majority of stability studies despite its restrictive assumptions. The plasma, modelled as a single fluid containing ions and electrons, is assumed to be at high temperature in order to avoid collisions which would go against the 1-fluid assumption. The ideal-MHD model, by opposition to the resistive-MHD model, makes the additional approximation that there is no plasma resistivity which eventually breaks down for too long time-scales. One specific characteristic of the ideal MHD model is that the plasma and the magnetic field are frozen together.

As explained in more clear steps below, the Grad-Shafranov equation is computed by combining Maxwell’s equations to the MHD equilibrium condition and is crucial for equilibrium description. In order to derive the Grad-Shafranov equation, we start from the Maxwell-Thomson law:

$$\nabla \cdot \mathbf{B} = 0 \quad (1)$$

to express the magnetic field components as functions of the poloidal magnetic flux ψ . The expression of the current density can then be derived from the Ampere law:

$$\nabla \wedge \mathbf{B} = \mu_0 \mathbf{J} \quad (2)$$

These expressions of \mathbf{B} and \mathbf{J} are then inserted into the force balance equation:

$$\mathbf{J} \wedge \mathbf{B} = \nabla P \quad (3)$$

which leads directly to the Grad-Shafranov equation (from papers [9], [10] and [11]). This equation will be used as rewritten in equation (31) of *COCOS* paper [3]:

$$\Delta^* \psi_{ref} = -\mu_0 R^2 p'(\psi) - TT'(\psi) = \mu_0 R j_\phi(R, Z) \quad (4)$$

2.2 CHEASE parameters

The CHEASE code needs two input profiles and boundary conditions to be specified in order to compute all the other equilibrium quantities by solving the Grad-Shafranov equation. The most common way to use CHEASE is to specify the pressure derivative p' and the surface average of the current density I^* . However, it would be very useful to rather give q instead of I^* in order to investigate the safety factor's influence on the equilibrium.

2.2.1 Definition of the safety factor q

The safety factor is defined as the ratio of toroidal over poloidal turns of the magnetic field lines. Let us start with its expression in equation (7) of the *COCOS* paper [3]:

$$q = \frac{1}{2\pi} \oint_{\psi=const} \frac{\mathbf{B} \cdot \nabla \phi}{\mathbf{B} \cdot \nabla \theta} d\theta \quad (5)$$

As q has the same value for all magnetic field lines on a given magnetic surface, it is only a function of the poloidal magnetic flux ψ , so:

$$q(\psi) = \frac{1}{2\pi} \oint_{\psi=const} \frac{1}{R} \frac{B_\phi}{B_p} dl_p \quad (6)$$

Where $B_\phi = \frac{T}{R}$, T being the poloidal current flux function, and $|B_p| = \frac{|\nabla \psi|}{R}$ are respectively the toroidal and poloidal magnetic fields and dl_p is the poloidal contour element. Hence:

$$q(\psi) = \frac{T(\psi)}{2\pi} \oint_{\psi=const} \frac{1}{R^2} \frac{dl_p}{B_p} \quad (7)$$

Where $\frac{dl_p}{B_p} = Jd\chi$, J being the Jacobian to go from the (ψ, χ, ϕ) non-orthogonal coordinates system to the Cartesian one. Using the expression of $C_2 = \oint_{s=const} \frac{1}{R^2} Jd\chi$ given in equation (9) of paper [2] *The CHEASE code for toroidal MHD equilibria*, we obtain the following expression for the safety factor:

$$\boxed{q(\psi) = \frac{T(\psi)}{2\pi} C_2(\psi)} \quad (8)$$

2.2.2 Definition of the toroidal current density j_ϕ and its surface average I^*

The expression of the toroidal current density j_ϕ is obtained from the Grad-Shafranov equation (4) which gives in CHEASE units:

$$j_\phi(R, Z) = -Rp'(\psi) - \frac{1}{R} TT'(\psi) \quad (9)$$

where CHEASE normalizes distances with R_0 and magnetic fields with B_0 . As explained in paper [6] *Normalizations on CHEASE*, if one uses the boundary condition $T_{CHEASE}(edge) = 1$, B_0 is then the vacuum magnetic field at $R = R_0$ such that $T(edge) = R_0 B_0$. The I^* surface averaged current can then be computed:

$$I^*(\psi) = \frac{\oint j_\phi(\psi) \frac{J}{R} d\chi}{\oint \frac{J}{R} d\chi} \quad (10)$$

$$= \frac{\oint [-Rp'(\psi) - \frac{1}{R}TT'(\psi)] \frac{J}{R} d\chi}{\oint \frac{J}{R} d\chi} \quad (11)$$

$$= \frac{1}{C_0} \left(-C_1 p'(\psi) - C_2 TT'(\psi) \right) \quad (12)$$

which corresponds to equation (7) of paper [2]. The surface integrals C_i , $i = 0, 1, ..4$, are defined in equation (9) of this same paper as:

$$\{C_0(s), C_1(s), C_2(s), C_3(s)\} = \oint_{s=const} \left\{ \frac{1}{R}, 1, \frac{1}{R^2}, \frac{|\nabla\psi|^2}{R^2} \right\} J d\chi \quad (13)$$

Now, using the definition of q from equation (8), we can replace the term TT' in the definition of I^* as $\left(\frac{q}{C_2}\right)'(\psi) = \frac{T'(\psi)}{2\pi}$ to obtain:

$$\boxed{I^*(\psi) = -\frac{C_1}{C_0} p'(\psi) - \frac{4\pi^2}{C_0} q(\psi) \left(\frac{q}{C_2}\right)'(\psi)} \quad (14)$$

3 Using a predefined q profile as CHEASE input with an external loop to find the appropriate I^* and TT' expressions

The safety factor profile is a crucial quantity for achieving stability in a tokamak. Indeed, depending on the value of its radial derivative at specific rational values, perturbations will either tend to grow or to vanish. It would therefore be very useful to be able to impose a specific q profile as CHEASE input in order to investigate its influence on the output equilibrium stability. The Grad-Shafranov equation (4) is non-linear in ψ as the functions p' and TT' both depend on ψ . Its resolution with CHEASE therefore requires an iterative numerical method in order to make it converge towards a solution.

Let us first explain the main idea behind the calculation performed in CHEASE. The numerical solving starts by initializing ψ and the coefficients C_i (13). A first "guess-computation" of ψ with a parabolic shape $\psi^0 = \psi_{guess}$ is made in order to

3 USING A PREDEFINED Q PROFILE AS CHEASE INPUT WITH AN EXTERNAL LOOP TO FIND THE APPROPRIATE I^* AND TT' EXPRESSIONS

Safety factor profile as CHEASE input

compute a first current density j_ϕ^0 and to test it within the Grad-Shafranov equation (4). A second profile ψ^1 is computed from solving the Grad-Shafranov equation with j_ϕ^0 to compute j_ϕ^1 which is then injected into the Grad-Shafranov equation...and so on until achieving convergence:

- p' & I^* as inputs \rightarrow first guess on $\psi^0 \rightarrow$ computation of Rj_ϕ^0 with equation (9)
- $\Delta\psi^1 = Rj_\phi^0(\psi^0) \rightarrow \psi^1 \rightarrow Rj_\phi^1$
- $\Delta\psi^2 = Rj_\phi^1(\psi^1) \rightarrow \psi^2 \rightarrow Rj_\phi^2$
- and so on...

Before implementing the new input case into the CHEASE code, external work has to be done in order to find the appropriate I^* expression which will lead to convergence towards the q profile we want. The aim of this whole section is to determine how to turn the safety factor profile we want into a fully consistent new equilibrium, that is to say to determine what input one needs in order to obtain a numerical answer which is consistent with our new q profile.

By recalling the Grad-Shafranov equation (4),

$$\Delta^* \psi_{ref} = -\mu_0 R^2 p' - TT' = \mu_0 R j_\phi$$

it appears that the two easiest input profiles to give are respectively the derivative of the pressure p' and the product of the poloidal current flux function with its derivative TT' . This corresponds to the case NSTTP=1. However other options are implemented in CHEASE which allow to rather give the toroidal surface average of the current density I^* (case NSTTP=2) or the parallel one I_\parallel (case NSTTP=3). Our goal here is to create a new case where we can replace TT' directly by the safety factor profile q . There are two ways to do that: one can either impose it through the surface averaged current density profile I^* or through TT' . Ideally, these two options would give similar answer but if this is not the case, one can determine which one is more suitable than the other. However, as stated in note [1], the relations between q and I^* or between q and TT' involve metric coefficients, the C_i , characterizing the equilibrium which means that they are different for each numerical iteration. One therefore has to choose very carefully the combination of *old* and *new* coefficients to compute the right CHEASE inputs in order to obtain a consistent equilibrium in output with $q_{out} = q_{in}$. Our aim is to obtain the equilibrium quantities C_i corresponding to an equilibrium where $q = q_{target}$.

3.1 I^* as the surface average of the current density j_ϕ

It turns out that it has been a long process to find a non-diverging I^* expression whilst imposing the safety factor profile. The first choice was naturally to use the expression (14) derived above:

$$I^*(\psi) = -\frac{C_1}{C_0} p'(\psi) - \frac{4\pi^2}{C_0} q(\psi) \left(\frac{q}{C_2} \right)'(\psi) \quad (15)$$

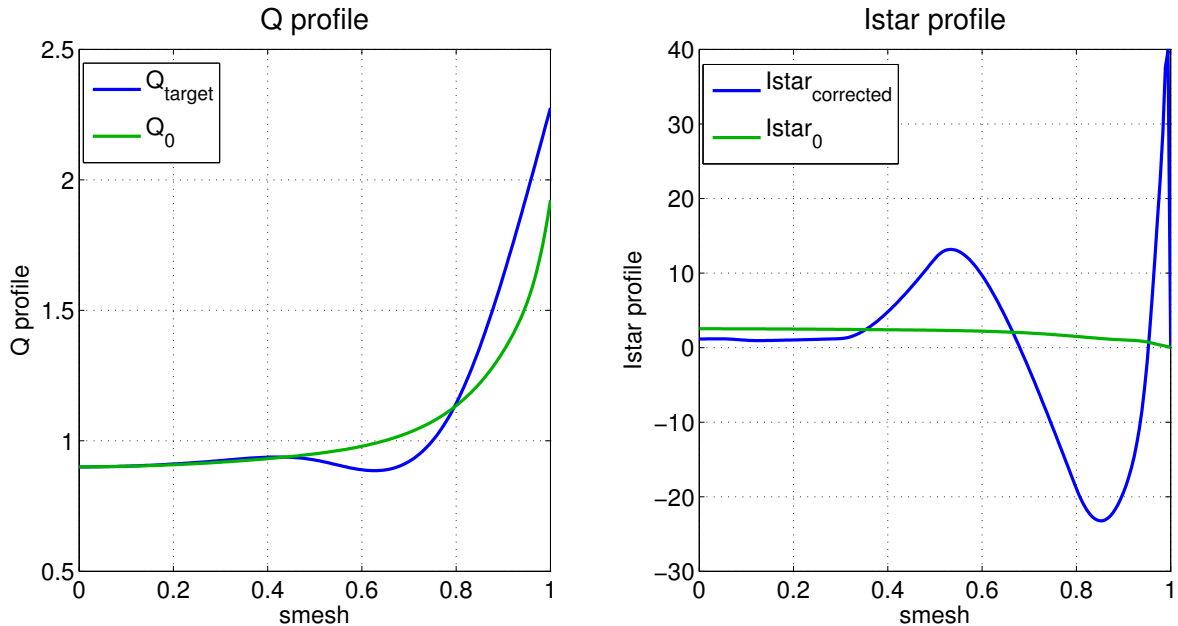


Figure 1: On the right graph, the initial I^* expression (drawn in green) has been updated with the q_{target} profile (blue curve on left graph). The resulting I^* expression is drawn in blue.

and to try different ways of using it, namely with different radial coordinates or different combination of *old* and *new* quantities. The main options tested which led to some improvements or which will be referred to later on in the text are presented below while the other ones can be consulted in details in the appendices.

Until stated differently, the runs have been carried out starting from an EXPEQ.OUT file, generated by the CHEASEgui tool, using the mesh of the radial coordinate:

$$\rho_{poloidal} = \sqrt{\frac{\psi}{\psi_{min}}}$$

An other option which will be tried below is to start from the EXPEQ.OUT.TOR file and to use the quantities with respect to $\rho_{toroidal}$.

In order to impose the desired safety factor profile (referred to as the "targeted profile") through equation (15), one started by updating all the q terms to q_{target} . However, as shown in figure 1, the corrections induced on the new current density profile $I^*_{corrected}$ are far bigger than needed. Indeed, as I^* evolves as $\frac{1}{q}$, we should observe almost the same changes in amplitude from q to q_{target} than from I_0^* to $I^*_{corrected}$. However the bump in I^* supposedly corresponding to the bump in q is far too important, which leads to another opposite huge bump in order to conserve the total current. Receiving this profile as input, CHEASE cannot even run because it does not make any physical sense to have a large negative surface averaged current density profile.

An option, detailed in appendix A, was to update either one of the two q terms of equation (15). However, regarding the failure of this test, this work directly moves

on to the next option while only keeping in mind that the derivative term:

$$\frac{d}{d\psi} \left(\frac{q}{C_2} \right)$$

is the one to be worked on.

3.1.1 Combining *old* and *new* I^* expressions

Another attempt to limit the correction induced in the I^* curve was to gradually update the input profile. That is to say to use only a small percentage of I_{target}^* and a majority percentage of I_{n-1}^* resulting from the last run by introducing a variable α such that:

$$I_{input,n}^* = \alpha \cdot I_{target}^* + (1 - \alpha) \cdot I_{n-1}^* \quad (16)$$

Since the I_{target}^* has huge oscillations (as shown in figure 1), the α has to be really small to avoid the curve of the current density to become negative which of course jeopardizes any chance of achieving convergence since it is not physically realistic. With an $\alpha = 0.05$, and so an input I^* corresponding to the red curve of figure 2, CHEASE runs and gives very correct first results, as shown in figure 3a. However the I^* profile starts rapidly to oscillate (figure 3b) and this has a knock-on effect on the safety factor profile, especially at the center. Indeed for a given flux surface, the safety factor not only depends on the current density j_ϕ on this surface but also on all the inner surfaces. Therefore q is very sensitive to current variations at the center but less and less while approaching the edge. The oscillations of the I^* profile near the center from the second run have therefore very bad consequences on the safety factor profile and make it impossible to obtain a consistent equilibrium.

3.1.2 Using an alternative radial coordinate

This option was motivated by looking more carefully at the respective evolution of the two radial coordinates accessible to us to do our calculations: $\rho_{poloidal}$ (corresponds to graph label SMESH) and $\rho_{toroidal}$ being respectively defined as:

$$\rho_{poloidal} = \sqrt{\frac{\psi}{\psi_{min}}} \quad (17)$$

$$\rho_{toroidal} = \sqrt{\frac{\Phi}{\pi B_0}} \quad (18)$$

where ψ_{min} is the first value of ψ , ie on the axis. Their respective evolutions over the runs are visible in figure 4 and while the variations of $\rho_{poloidal}$ appear clearly, $\rho_{toroidal}$ remains nearly constant and seems therefore to be a better spatial coordinate for our calculation. Indeed, the toroidal spatial coordinate is a function of the toroidal magnetic flux Φ :

$$\Phi = \oiint B_\phi dS_\phi = \oiint \frac{T(\psi)}{R} dS_\phi \quad (19)$$

3.1 I^* as the surface average of the current density profile as CHEASE input

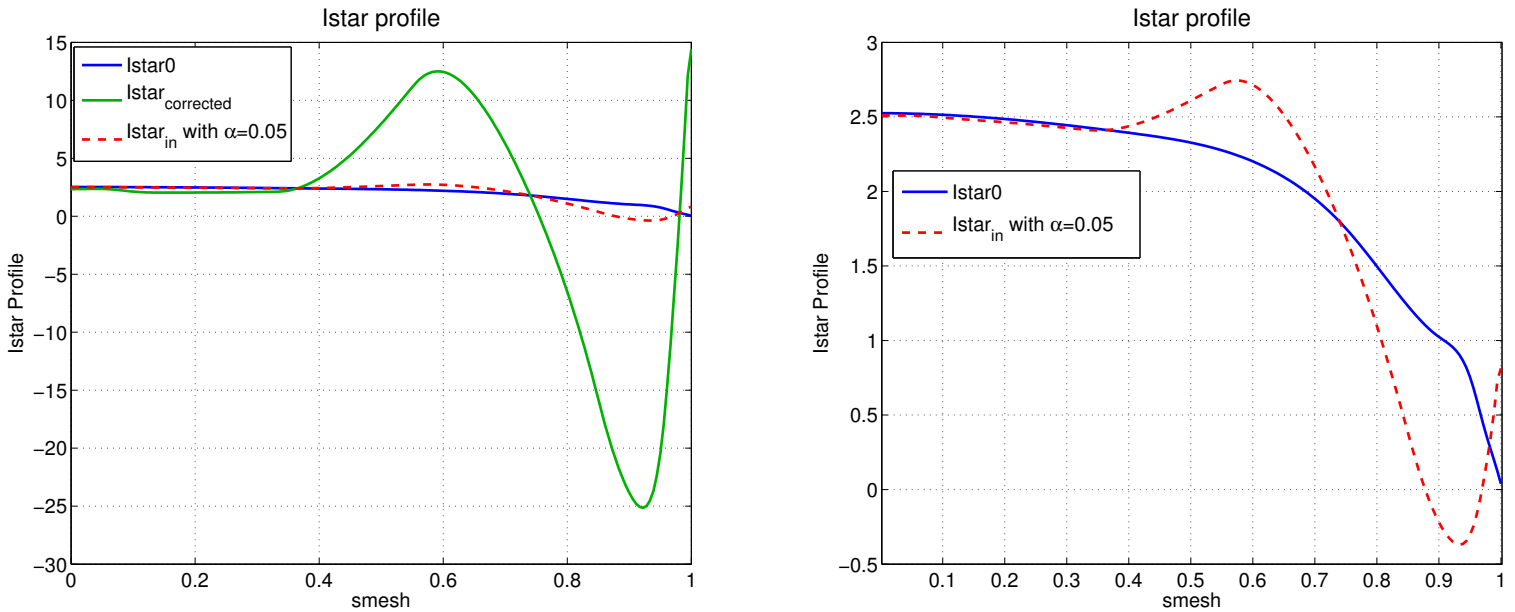


Figure 2: Computation of a decent I^* input profile (red dashed curve) from 95% of I_0^* and 5% of I_{new}^* without imposing a special boundary condition.

where T denotes the poloidal current flux function whose value remains around 1. The toroidal magnetic field B_ϕ which is highly dominant compared to the poloidal magnetic field has a $1/R$ -dependence and is maximum at the center of the torus and does not vary much across the plasma area. The Φ value is therefore not really dependent on the change of the plasma current density profile and remains almost equal to:

$$\Phi \approx \oiint B_0 dS_\phi \quad (20)$$

On the contrary, the poloidal spatial coordinate is directly linked to ψ which measures the flux of poloidal magnetic field. As B_p is generated by the plasma current, ψ is sensitive to changes of the current density profile over the iterations.

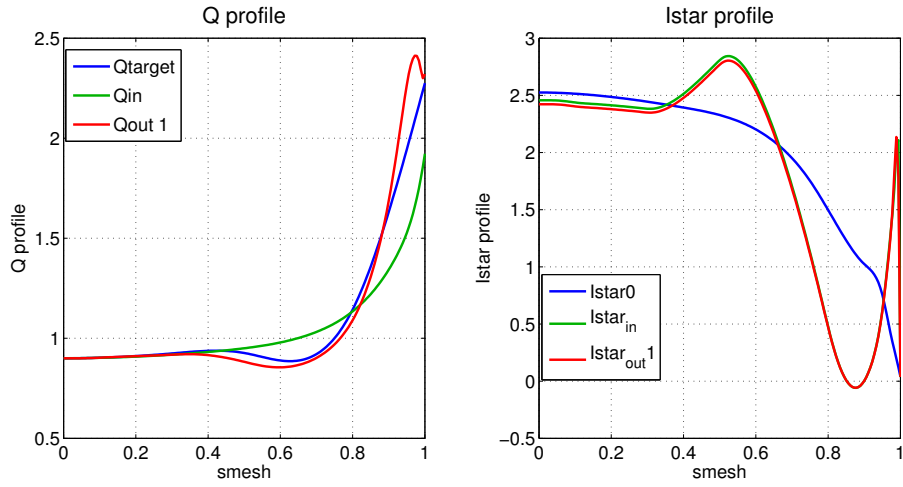
Hence input I^* will be tested in this section using the radial coordinate $\rho_{toroidal}$ instead of $\rho_{poloidal}$. This means that we give the file EXPEQ.TOR as input and that the namelist coefficient NFUNRHO is changed to 1. Note that the input TT' is not compatible with using NFUNRHO=1: if attempted, the calculation diverges immediately and is aborted.

The improvement is immediately visible in figure 35 (presented in appendix D) compared to figure 3 as the bump at the edge finally disappeared from the safety factor profile. However, despite this improvement, the current density profile is still oscillating which does not allow the calculation to go further than run 3.

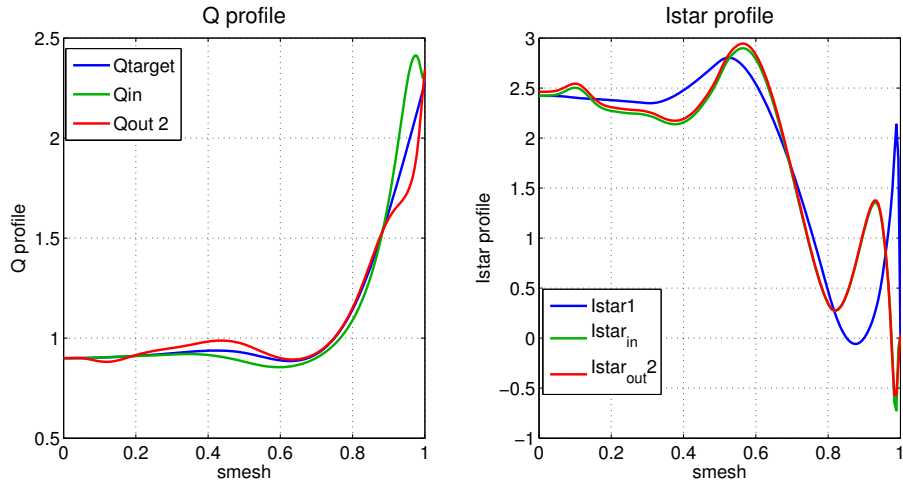
At this point lots of tests and efforts have been made working on the expression (15) of I^* . Despite the improvements which allow now CHEASE to run, namely using α and switching the radial coordinate, an input expression allowing conver-

3 USING A PREDEFINED Q PROFILE AS CHEASE INPUT WITH AN EXTERNAL LOOP TO FIND THE APPROPRIATE I^* AND TT' EXPRESSIONS

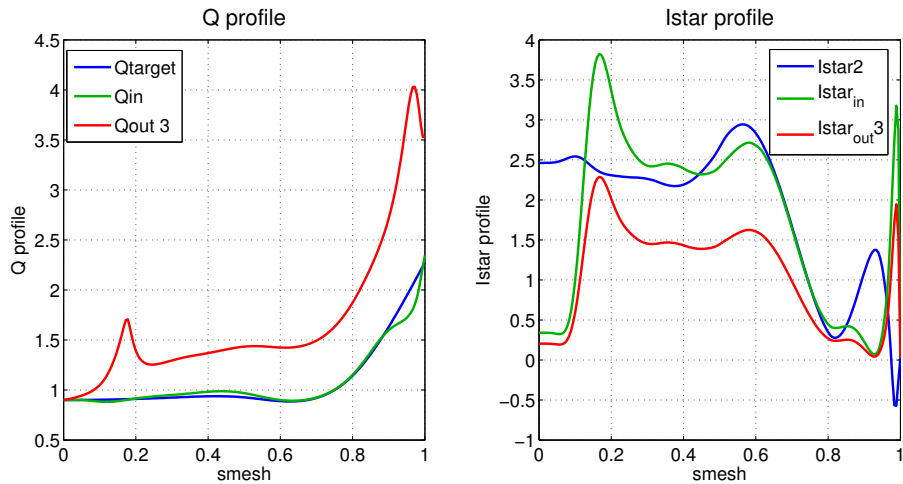
Safety factor profile as CHEASE input



(a) First run with input $I^*(q)$ and $\alpha = 0.05$



(b) Second run with input $I^*(q)$ and $\alpha = 0.05$



(c) Third run with input $I^*(q)$ and $\alpha = 0.05$

Figure 3: Q and I^* profiles after a few runs of CHEASE using input I^* formula (15). Even though the first run output seems quite good except for the bump at the edge of the safety factor profile, the next run shows the profiles to start oscillating and diverging. Run done with $\alpha = 0.05$ and $\text{NFUNRHO}=0$ (ie with ρ_{poloidal}).

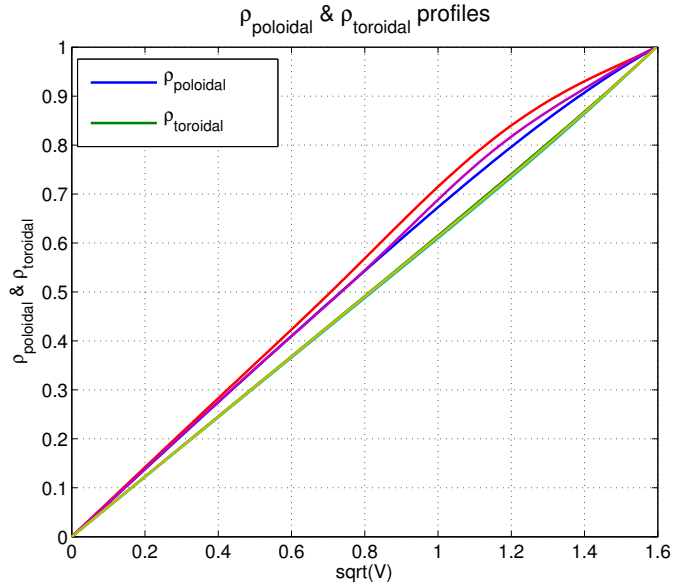


Figure 4: Evolution of the two radial coordinates ρ_{poloidal} & ρ_{toroidal} over three runs of CHEASE with respect to the stable quantity \sqrt{V} .

gence towards the targeted safety factor profile has still not been established. It is therefore time to try another input expression which leads us to the next section.

3.2 $TT'(q)$ as input instead of $I^*(q)$

Another way of specifying q in input would be through the TT' quantity, using expression (8) reminded below:

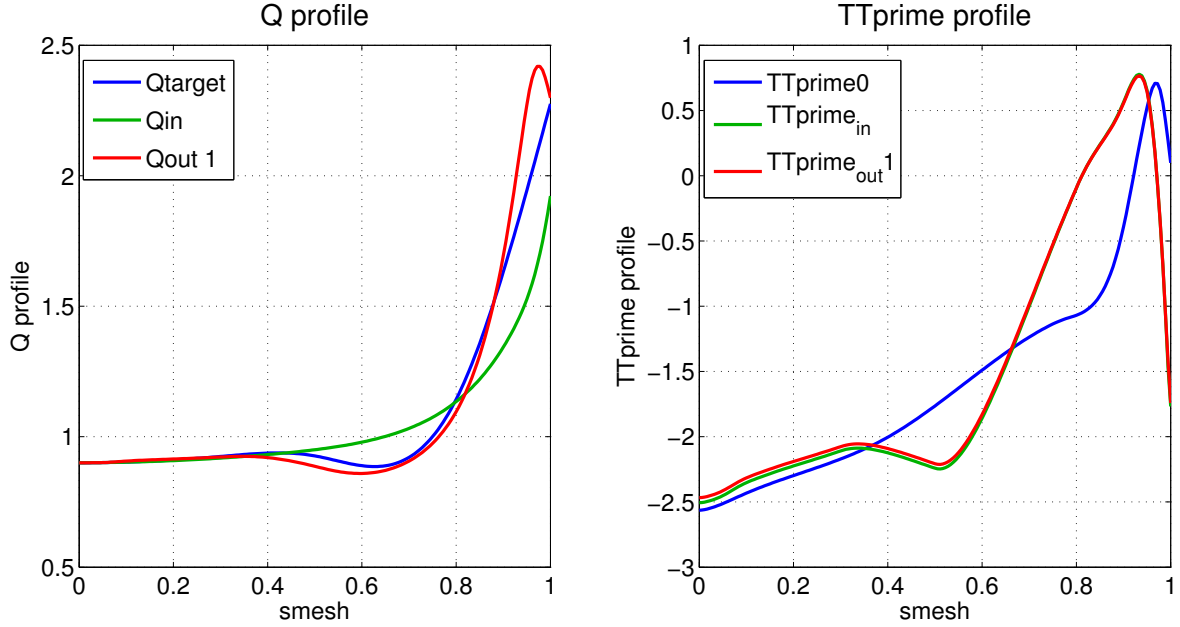
$$T = 2\pi \frac{q}{C_2}$$

which leads directly to the expression of TT' (21):

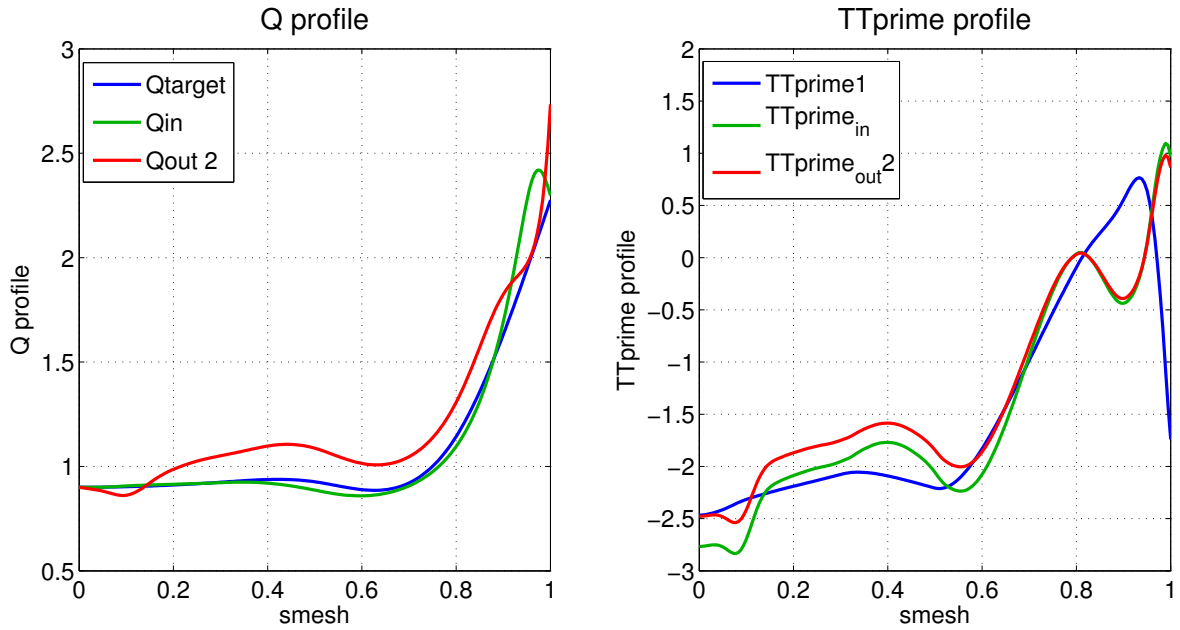
$$TT'_{\text{target}} = 4\pi^2 \frac{q_{\text{target}}}{C_2} \frac{d}{d\psi} \left[\frac{q_{\text{target}}}{C_2} \right] \quad (21)$$

The first run results, presented in figure 5a, are as good as the one using input $TT'(I^*)$ (shown in appendix C) although no special boundary condition have been used here. However, similar oscillations start from the second run (figure 5b) and make the third run's attempt fail. This input expression (21) was motivated by the fact that it was no longer depending on p' which contribution is not negligible at all at the center and at the edge and could have been responsible for the central bump. However, the same oscillation problem remains with the computation of the derivative term $\frac{d}{d\psi} \left(\frac{q}{C_2} \right)$.

The fact that this option is not conclusive dismisses the idea of implementing a case NSTTP = 6 where TT' would be calculated directly as a function of the input q



(a) First run with input $TT'(q)$ and $\alpha = 0.05$



(b) Second run with input $TT'(q)$ and $\alpha = 0.05$

Figure 5: Q and TT' profiles after a few runs of CHEASE using input TT' expression $TT'_n = \alpha \cdot TT'_{target} + (1 - \alpha) \cdot TT'_{n-1}$ (where TT'_{target} comes from expression (21) and TT'_{n-1} is the output profile of the previous run). Run made without any special boundary condition, with $\alpha = 0.05$ and $NFUNRHO=0$.

profile. From here on the focus will then be to find an appropriate I^* expression for the implementation of the case NSTTP = 5.

3.3 I^* from Antoine Merle's note

While still being the surface average of the toroidal current density, I^* will be approached differently in this section as the derivative of the plasma current I_p with respect to ψ . The plasma current is known to be the surface integral of the toroidal current density j_ϕ and can therefore be expressed as:

$$I_p = \oiint j_\phi dS_\phi \quad (22)$$

$$= \oiint j_\phi \frac{d\psi}{|\nabla\psi|} dl_p \quad (23)$$

$$= \oiint j_\phi \frac{d\psi}{|\nabla\psi|} B_p \frac{dl_p}{B_p} \quad (24)$$

$$= \oiint j_\phi \frac{d\psi}{|\nabla\psi|} \frac{|\nabla\psi|}{R} J d\chi \quad (25)$$

Hence, with the expression of $C_0 = \oint_{s=const} \frac{1}{R} J d\chi$ from equation (13), and recalling that $I^*(s) = \frac{\oint_{s=const} j_\phi (\frac{J}{R}) d\chi}{\oint_{s=const} (\frac{J}{R}) d\chi}$ we obtain:

$$\frac{dI_p}{d\psi} = \oint j_\phi \left(\frac{J}{R} \right) d\chi \quad (26)$$

$$= I^*(\psi) \oint \left(\frac{J}{R} \right) d\chi \quad (27)$$

$$= I^*(\psi) C_0(\psi) \quad (28)$$

From this last expression, one can re-derive the expression of I^* used in the note written by Antoine Merle [1] by first expressing ψ as a function of ρ and the surface integral of $\frac{1}{R}$ as the ratio of C_0 over C_1 :

$$\left\langle \frac{1}{R} \right\rangle = \frac{\oint \frac{1}{R} \frac{dl_p}{B_p}}{\oint \frac{dl_p}{B_p}} = \frac{C_0}{C_1} \quad (29)$$

$$I^* = \frac{1}{C_0} \frac{dI_p(\rho(\psi))}{d\psi} \quad (30)$$

$$= \frac{1}{C_1} \frac{1}{\left\langle \frac{1}{R} \right\rangle} \frac{d\rho}{d\psi} \frac{dI_p}{d\rho} \quad (31)$$

$$= \frac{1}{\mu_0 \langle |\nabla\phi| \rangle} \left(\frac{1}{2\pi} \frac{dV}{d\psi} \right)^{-1} \frac{d\rho}{d\psi} \frac{d}{d\rho} [\mu_0 I_p] \quad (32)$$

$$(33)$$

since:

$$\frac{dV}{d\psi} = 2\pi C_1$$

To obtain the targeted expression inside the derivative term, one can use the Ampere law which links the poloidal magnetic field to its source: the plasma current.

$$\mu_0 I_p = \oint B_p dl_p = \oint B_p^2 \frac{dl_p}{B_p} = \langle B_p^2 \rangle \oint \frac{dl_p}{B_p} \quad (34)$$

$$= \langle B_p^2 \rangle C_1 = \langle B_p^2 \rangle \frac{dV}{d\psi} \frac{1}{2\pi} \quad (35)$$

$$= \left\langle \frac{|\nabla\psi|^2}{R^2} \right\rangle \frac{dV(\psi(\rho))}{d\psi} \frac{1}{2\pi} \quad (36)$$

$$= \left\langle \frac{|\nabla\rho|^2}{R^2} \left(\frac{d\psi}{d\rho} \right)^2 \right\rangle \frac{dV}{d\rho} \frac{d\rho}{d\psi} \frac{1}{2\pi} \quad (37)$$

$$= \frac{1}{2\pi} \frac{dV}{d\rho} \left\langle \frac{|\nabla\rho|^2}{R^2} \right\rangle \frac{d\psi}{d\rho} \quad (38)$$

To re-arrange the outside terms of the derivative, one uses the fact that $|\nabla\Phi| = \frac{1}{R}$ and that $\left(\frac{1}{2\pi} \frac{dV(\rho(\psi))}{d\psi} \right)^{-1} = 2\pi \left(\frac{dV}{d\rho} \right)^{-1} \frac{d\psi}{d\rho}$. This leads directly to the expression of I^* used in note [1]:

$$I^* = \frac{\sigma_{B_p}}{(2\pi)^{e_{B_p}}} \frac{1}{\mu_0 \langle |\nabla\Phi| \rangle} \left(\frac{dV}{d\rho_{tor}} \right)^{-1} \frac{d}{d\rho_{tor}} \left(\frac{dV}{d\rho_{tor}} \left\langle \left| \frac{\nabla\rho_{tor}}{R} \right|^2 \right\rangle \frac{d\psi}{d\rho_{tor}} \right) \quad (39)$$

where only $\frac{d\psi}{d\rho_{tor}}$ will be the only updated quantity. The ρ quantity used all along is the previous calculation refers to the toroidal spatial coordinate $\rho_{toroidal}$. Note that the *COCOS* convention used here is the second one for which $\sigma_{B_p} = 1$ and $e_{B_p} = 0$. In order to express the updated quantity $\frac{d\psi}{d\rho_{tor}}$ one has to start from equation (9) of the *COCOS* paper [3]:

$$q = \frac{\sigma_{B_p} \sigma_{\phi\theta\rho}}{(2\pi)^{(1-e_{B_p})}} \frac{d\Phi_{tor}}{d\psi_{ref}} \quad (40)$$

which will be from here on expressed in the *COCOS 2* convention. In order to compute a correct expression, one has to carefully recall to use the CHEASE units which normalize distances with R_0 and magnetic fields with B_0 :

$$\Phi_{tor,CHEASE} = \frac{\Phi_{tor,physical}}{R_0^2 B_0} \quad (41)$$

$$\rho_{tor,CHEASE} = \frac{\rho_{tor,physical}}{R_0} \quad (42)$$

From the expression of $\rho_{tor} = \sqrt{\frac{\Phi_{tor}}{\pi B_0}}$, one can then compute the quantity $d\Phi_{tor}$ and

go on with the calculation:

$$R_0 \rho_{tor,CHEASE} = \sqrt{\frac{R_0^2 B_0 \Phi_{tor,CHEASE}}{\pi B_0}} \rightarrow \rho_{tor,CHEASE} = \sqrt{\frac{\Phi_{tor,CHEASE}}{\pi}} \quad (43)$$

The safety factor is then computed from equation (40):

$$q_{CHEASE} = \frac{1}{2\pi} \frac{d\Phi_{tor,CHEASE}}{d\psi_{CHEASE}} \quad (44)$$

$$= \frac{1}{2\pi} \frac{(2\pi \rho_{tor,CHEASE} d\rho_{tor,CHEASE})}{d\psi_{CHEASE}} \quad (45)$$

From here on the label "CHEASE" will be implicit and the quantity updated in the expression (39) of I^* will write:

$$\left(\frac{d\psi}{d\rho_{tor}} \right)_{updated} = \frac{\rho_{tor}}{q_{target}} \quad (46)$$

Using the new I^* expression (39) directly as input (NSTTP = 2) or through

$$TT' = -\frac{C_0}{C_2} I^* - \frac{C_1}{C_2} p' \quad (\text{NSTTP} = 1)$$

leads immediately to stunning improvements. The first five runs of both input options are presented respectively in figures 6 and 36 (the latter can be consulted in appendix E) and convergence is achieved for both cases. The convergence is reached without any oscillation or bump towards a perfectly consistent equilibrium with a safety factor corresponding to the targeted one. Moreover, the exact same results are observed when running with either $\rho_{poloidal}$ (NFUNRHO=0) or $\rho_{toroidal}$ (NFUNRHO=1). However, the expression (39) is really meant to be used as written, only with the ratio (46) being an updated quantity. If used differently, the results can vary significantly.

The convergence of expression (39) is mainly achieved because some terms compensate the others. For example, the poloidal magnetic field sets a zero-value for the inner-integral term at the center and it would have been less steady with another combination of terms. Expression (39) has been re-arranged for simplicity purposes when will come the time of its implementation inside the CHEASE code. Having to deal mainly with the already existing variables, the following final expression will be used from here on:

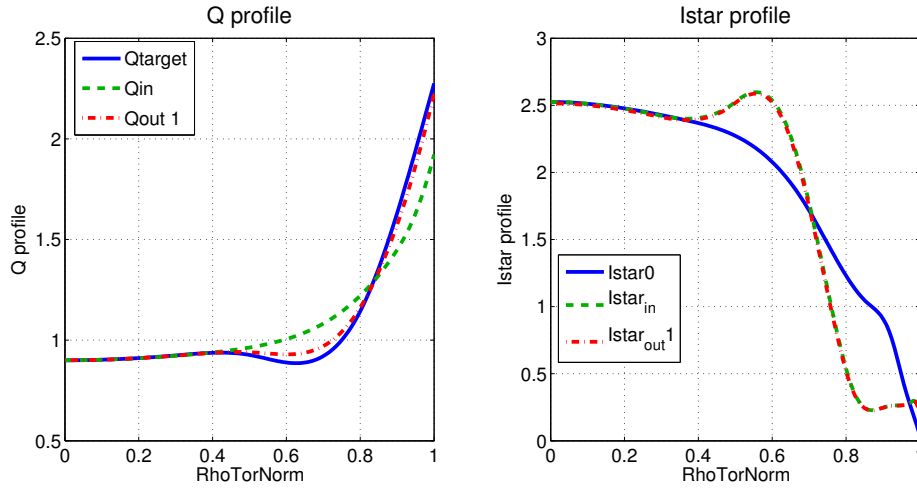
$$I^* = \frac{1}{\langle \frac{1}{R} \rangle} \left(\frac{dV}{d\rho} \right)^{-1} \frac{d}{d\rho} \left(\frac{dV(\rho(\psi))}{d\rho} \left\langle \left| \frac{\nabla \rho}{R} \right|^2 \right\rangle \frac{d\psi}{d\rho} \right) \quad (47)$$

$$= \frac{1}{\langle \frac{1}{R} \rangle} \left(\frac{dV}{d\rho} \right)^{-1} \frac{dV}{d\rho} \frac{d}{dV} \left(\frac{dV}{d\psi} \frac{d\psi}{d\rho} \left\langle \left(\frac{d\rho}{d\psi} \right)^2 \left| \frac{\nabla \psi}{R} \right|^2 \right\rangle \frac{d\psi}{d\rho} \right) \quad (48)$$

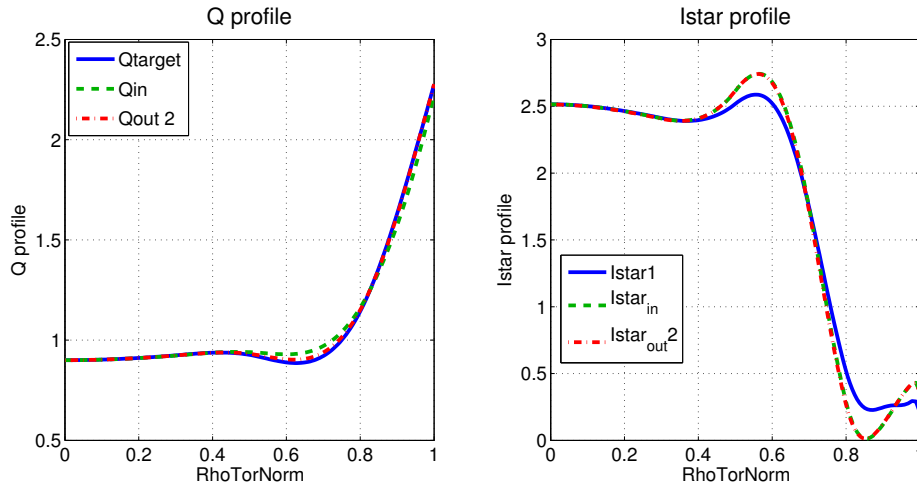
$$= \frac{1}{\langle \frac{1}{R} \rangle} \left(\frac{dV}{d\psi} \right)^{-1} \frac{d}{d\psi} \left(\frac{dV}{d\psi} \frac{d\rho}{d\psi} \langle B_p^2 \rangle \frac{d\psi}{d\rho} \right) \quad (49)$$

3 USING A PREDEFINED Q PROFILE AS CHEASE INPUT WITH AN EXTERNAL LOOP TO FIND THE APPROPRIATE I^* AND TT' EXPRESSIONS

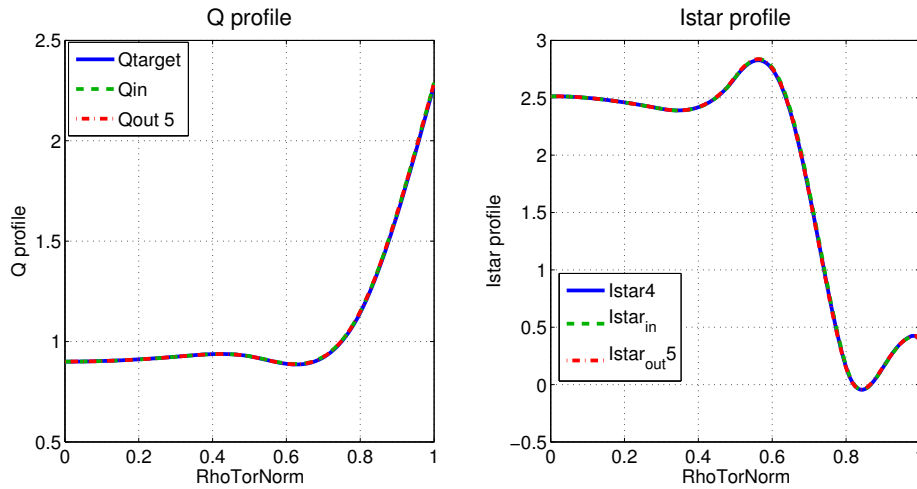
Safety factor profile as CHEASE input



(a) First run with input $I^*(q)$ (39)



(b) Second run with input $I^*(q)$ (39)



(c) Fifth run with input $I^*(q)$ (39)

Figure 6: Input I^* , NSTTP=2, NFUNRHO=0, $\alpha = 1$. Q and I^* profiles after a few runs of CHEASE using input I^* formula (39). The graphs show that the solution is steadily converging and leads to very good results.

$$I^* = \frac{1}{\langle \frac{1}{R} \rangle} \left(\frac{dV}{d\psi} \right)^{-1} \frac{d}{d\psi} \left(\frac{dV}{d\psi} q \langle B_p^2 \rangle \frac{1}{q_{target}} \right) \quad (50)$$

where B_p refers to the poloidal magnetic field. This expression (50) given as such in input gave exactly the same very good convergence results as shown in figure 6. Some tests with specific safety factor shapes will be conducted in the next section in order to approve this expression to be implemented as option NSTTP = 5 in CHEASE. Note that the choice of keeping the term

$$\left(\frac{dV}{d\psi} \right)^{-1} \frac{d}{d\psi}$$

untouched instead of calculating directly the derivative with respect to V has been made for convenience purposes. Indeed, while the term

$$\left(\frac{dV}{d\psi} \right)$$

is directly accessible in the code via the coefficient C_1 and the derivative with respect to ψ can be easily computed, the volume V is not directly accessible for the calculation where one wants to implement the calculation for $I^*(q)$.

3.4 Testing specific q profiles

3.4.1 First profile

The first profile, drawn on the right graph of figure 7, is in fact the one which has been used all along in the previous section to find the appropriate I^* expression. The EXPEQ file given in input is shown on the left graph of figure 7 and the outputs of runs one to five were presented above in figure 6.

3.4.2 Series of four profiles

The aim of this section is to test the I^* expression (50) found in section 3.3 on a four-profiles-series with a circular plasma shape. Also being in the large aspect ratio approximation (as $\frac{R_0}{a} = 20$), the surface averaged current density should be equal to the averaged parallel current density, which means that one should find $I^* = I_{\parallel}$. The general expressions for the safety factor and for the expected I_{\parallel} are written below in equations (51) and (52). Depending on the case studied, p_i will either be equal to 1, 2, 4 or 8.

$$q_{target,i} = q_0 \left(1 + \left(\frac{\rho}{\alpha} \right)^{2p_i} \right)^{\frac{1}{p_i}} \quad (51)$$

$$I_{\parallel,i} = \frac{I_0}{\left(1 + \left(\frac{\rho}{\alpha} \right)^{2p_i} \right)^{\left(1 + \frac{1}{p_i} \right)}} \quad (52)$$

3 USING A PREDEFINED Q PROFILE AS CHEASE INPUT WITH AN EXTERNAL LOOP TO FIND THE APPROPRIATE I^* AND TT' EXPRESSIONS

Safety factor profile as CHEASE input

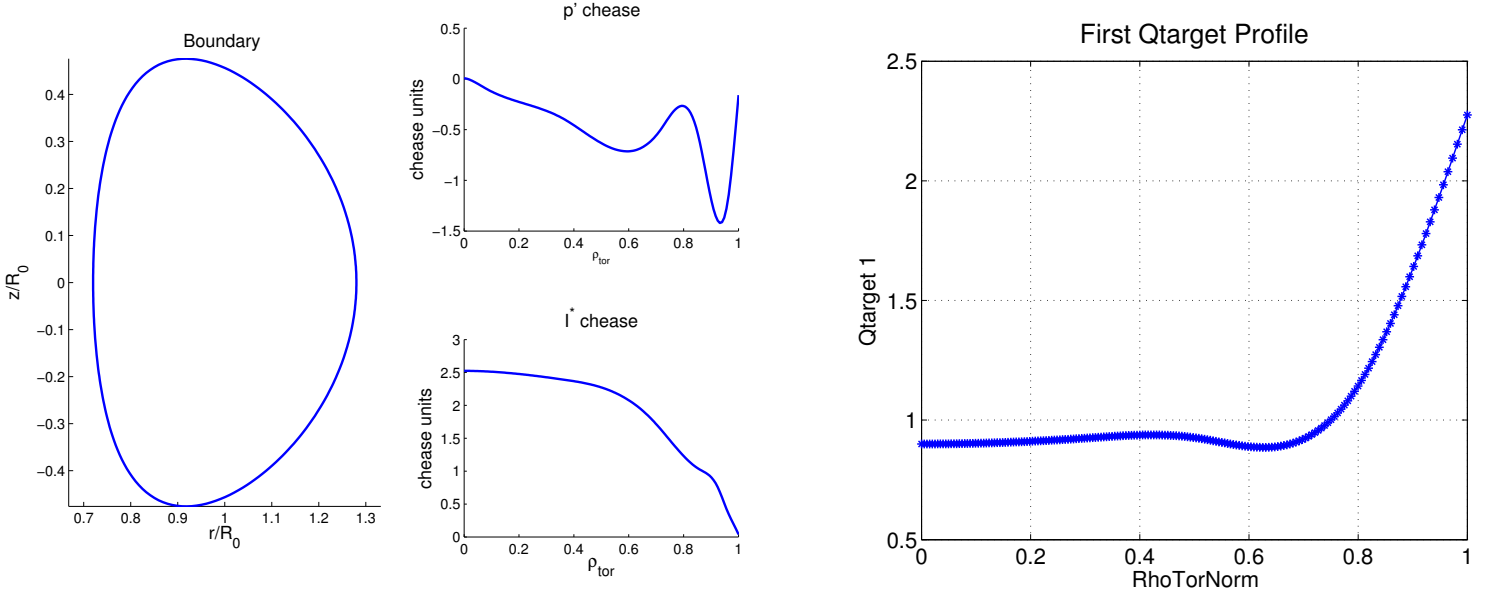


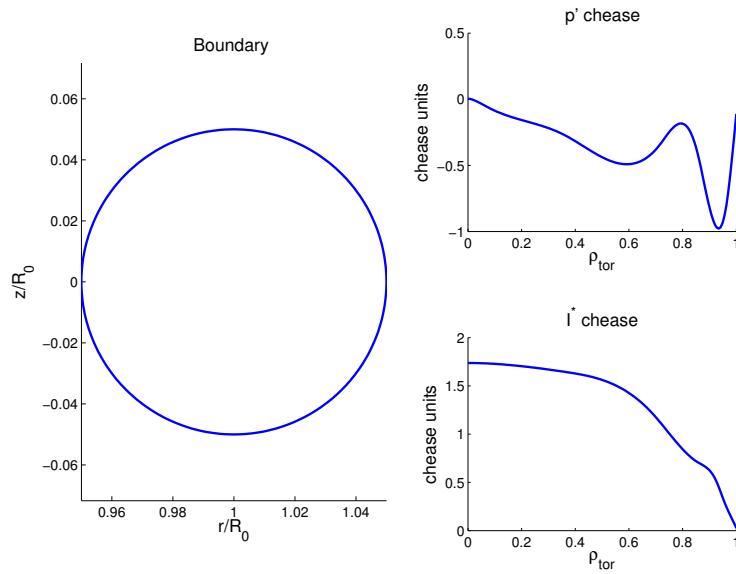
Figure 7: First targeted safety factor profile and the EXPEQ file given in input.

Where:

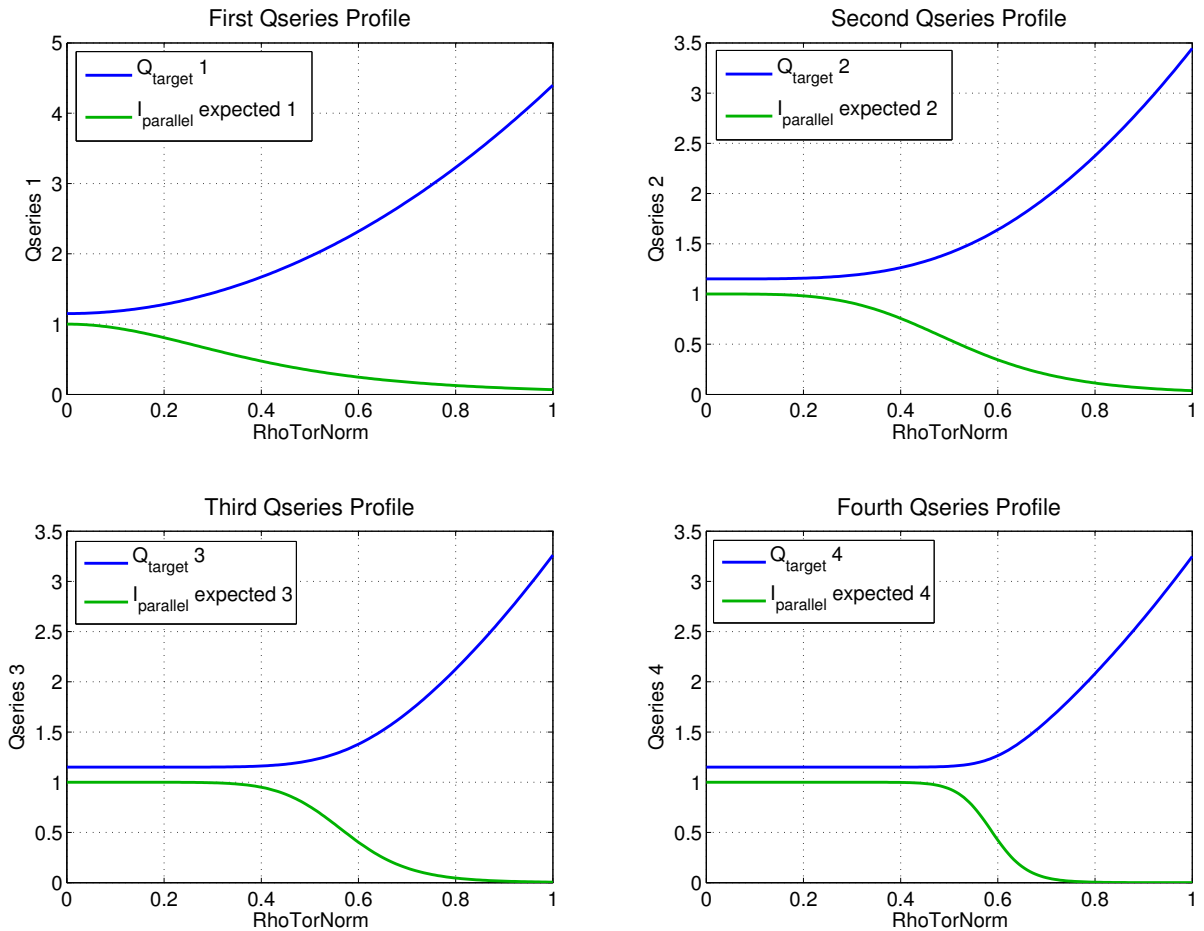
$$\left\{ \begin{array}{l} \rho = \rho_{tor,norm} \\ \alpha_0 = 0.595 \\ R_{0,exp} = 10 \\ a_{minor} = 0.5 \\ q_0 = 1.15 \end{array} \right. \quad (53)$$

$$\left\{ \begin{array}{l} q_{target,1} \rightarrow p_1 = 1 \\ q_{target,2} \rightarrow p_2 = 2 \\ q_{target,3} \rightarrow p_3 = 4 \\ q_{target,4} \rightarrow p_4 = 8 \end{array} \right. \quad (54)$$

The respective ten first runs corresponding to each one of the four profiles are presented in figures 9, 10, 11 and 12. The first computation of I^* from expression (50) corresponds indeed to the expected expression for I_{\parallel} (with $I_0 = I^*(1)$) and the output current density profile remains constant over the runs. The first output safety factor corresponds for each case to the targeted one and remains converged over the runs. This expression of I^* is therefore validated for this series of profiles too by leading immediately to the equilibrium we were looking for. Note that CHEASE computation's time is shorter for those target-profiles than for the one tested above.



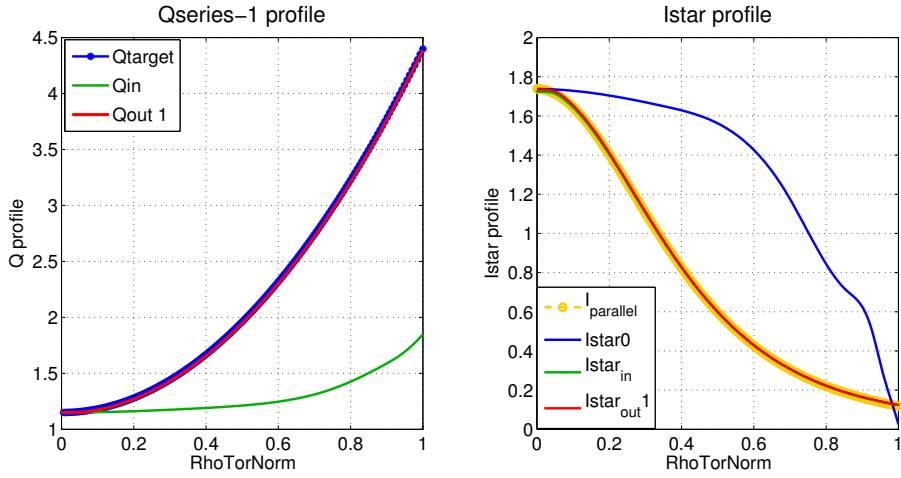
(a) Input EXPEQ file for the series of four profiles. Note that the plasma boundary is circular in those cases with a large aspect ratio (20).



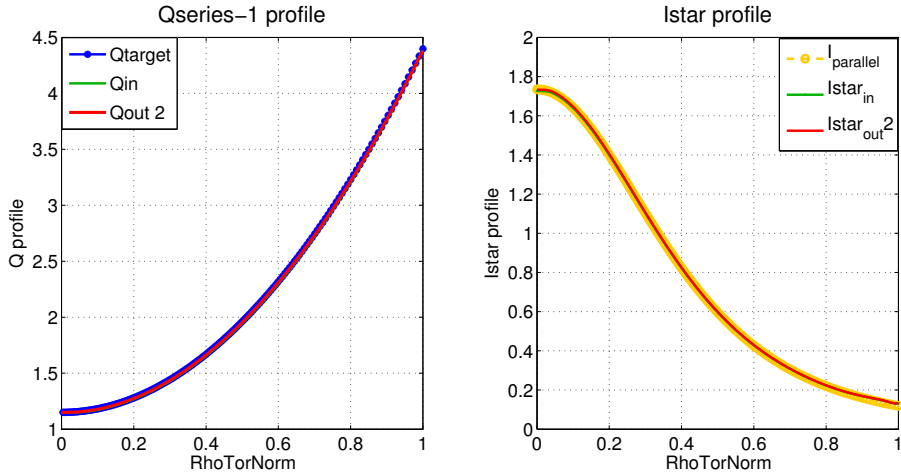
(b) Plot showing the four profiles of the series and their respective expected I_{\parallel} (with $I_0 = 1$) profiles which can be approximated to I^* in large aspect ratio.

3 USING A PREDEFINED Q PROFILE AS CHEASE INPUT WITH AN EXTERNAL LOOP TO FIND THE APPROPRIATE I^* AND TT' EXPRESSIONS

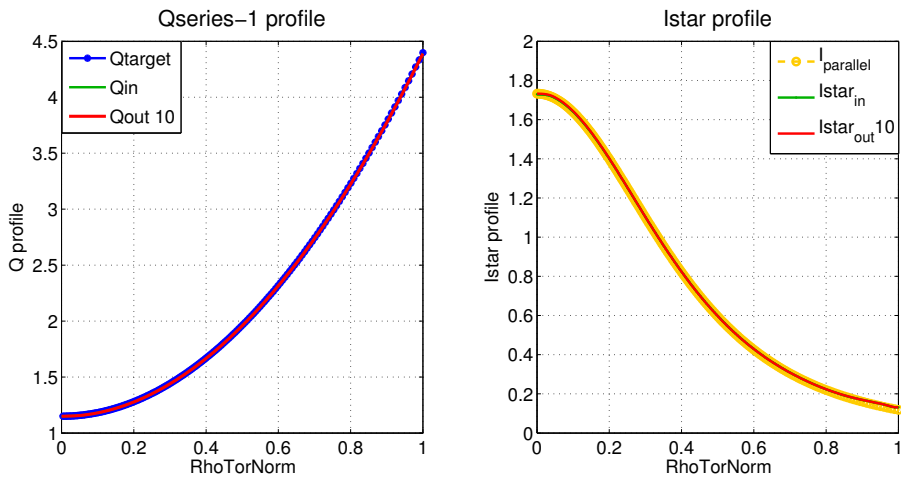
Safety factor profile as CHEASE input



(a) First q -series profile. Run 1.



(b) First q -series profile. Run 2.



(c) First q -series profile. Run 10.

Figure 9: First q -series profile. Run 1 to 10 using I^* input expression (50), NFUN-RHO=1, $\alpha = 1$. From the first run the output safety factor is very well superimposed to the target one and this convergence holds over the runs. The first computation of I^* using formula (50) already corresponds to the expected $I_{||}$ and so does the output profile.

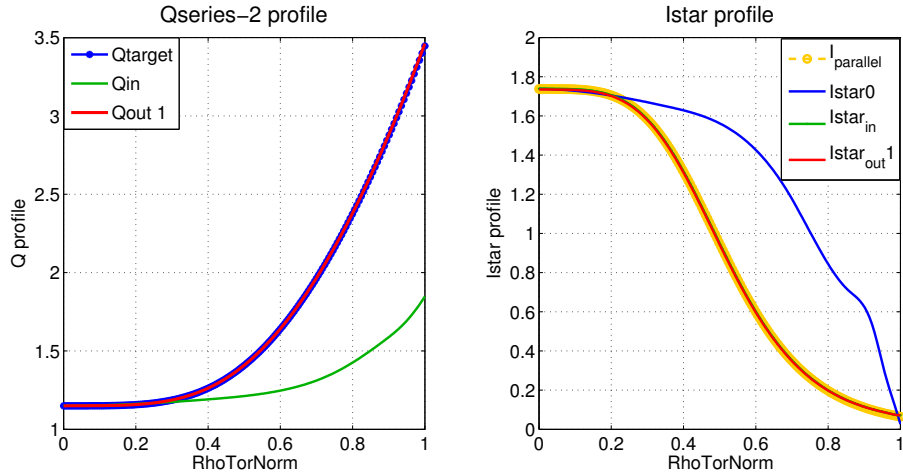
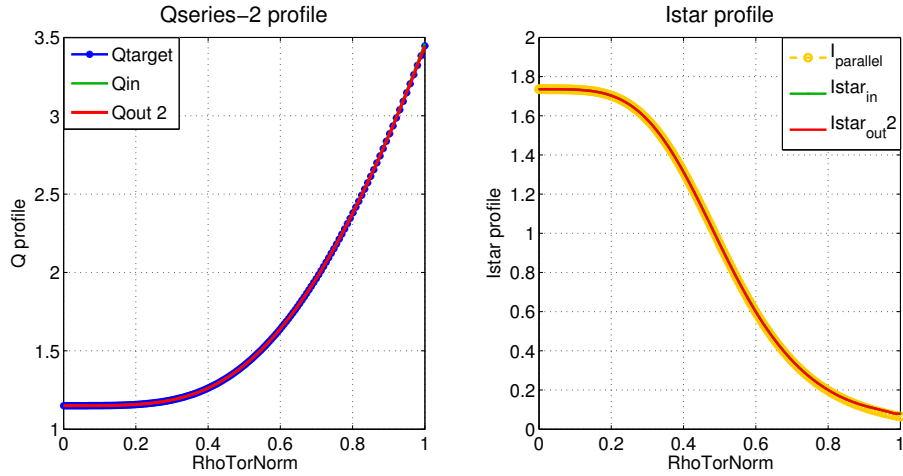
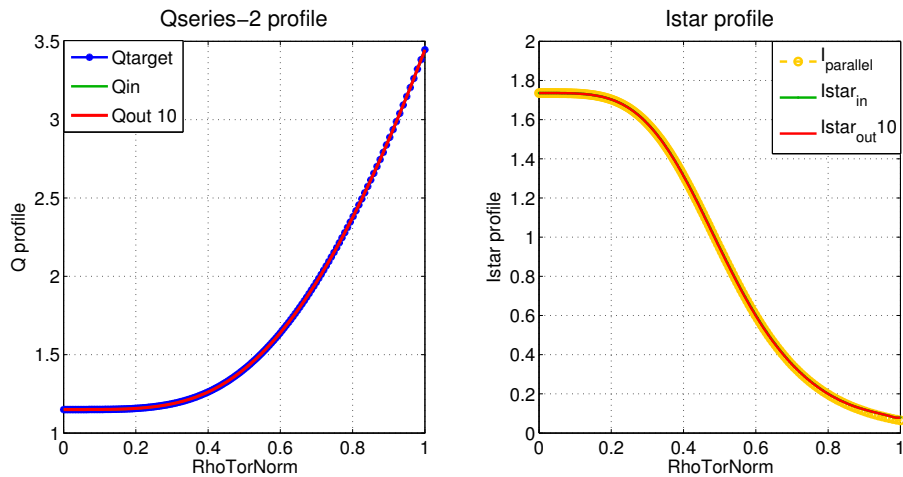
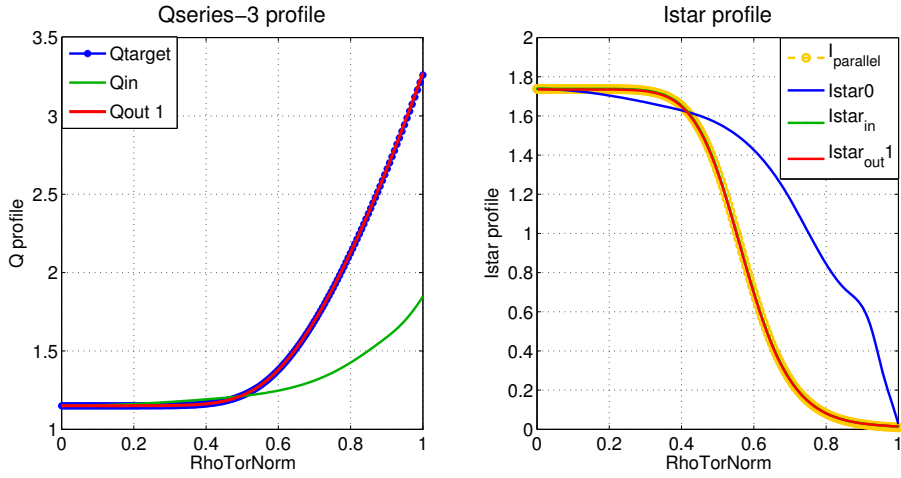
(a) Second q -series profile. Run 1.(b) Second q -series profile. Run 2.(c) Second q -series profile. Run 10.

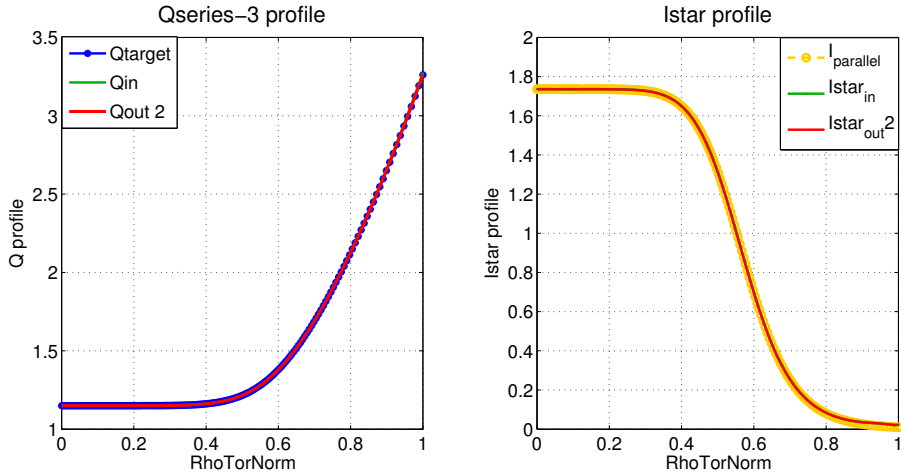
Figure 10: Second q -series profile. Run 1 to 10 using I^* input expression (50), $\text{NFUNRHO}=1$, $\alpha = 1$. From the first run the output safety factor is very well superimposed to the target one and this convergence holds over the runs. The first computation of I^* using formula (50) already corresponds to the expected I_{\parallel} and so does the output profile.

3 USING A PREDEFINED Q PROFILE AS CHEASE INPUT WITH AN EXTERNAL LOOP TO FIND THE APPROPRIATE I^* AND TT' EXPRESSIONS

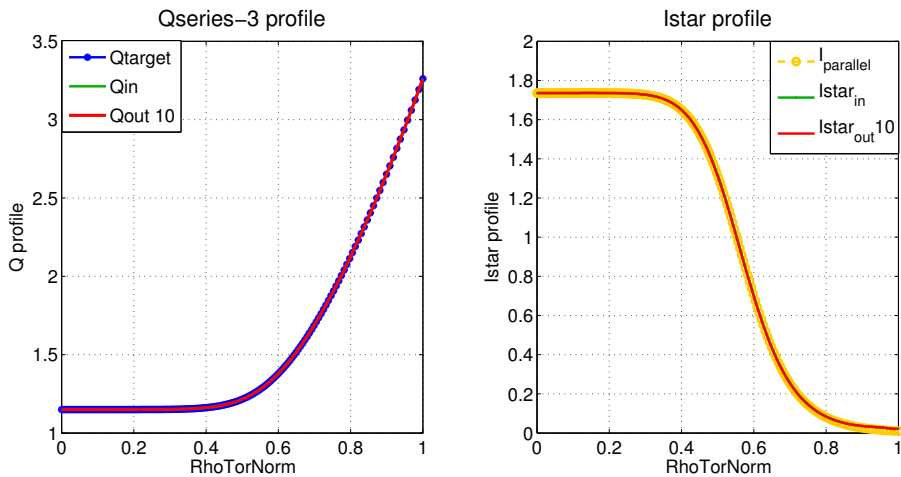
Safety factor profile as CHEASE input



(a) Third q -series profile. Run 1.



(b) Third q -series profile. Run 2.



(c) Third q -series profile. Run 10.

Figure 11: Third q -series profile. Run 1 to 10 using I^* input expression (50), NFUN-RHO=1, $\alpha = 1$. From the first run the output safety factor is very well superimposed to the target one and this convergence holds over the runs. The first computation of I^* using formula (50) already corresponds to the expected I_{\parallel} and so does the output profile.

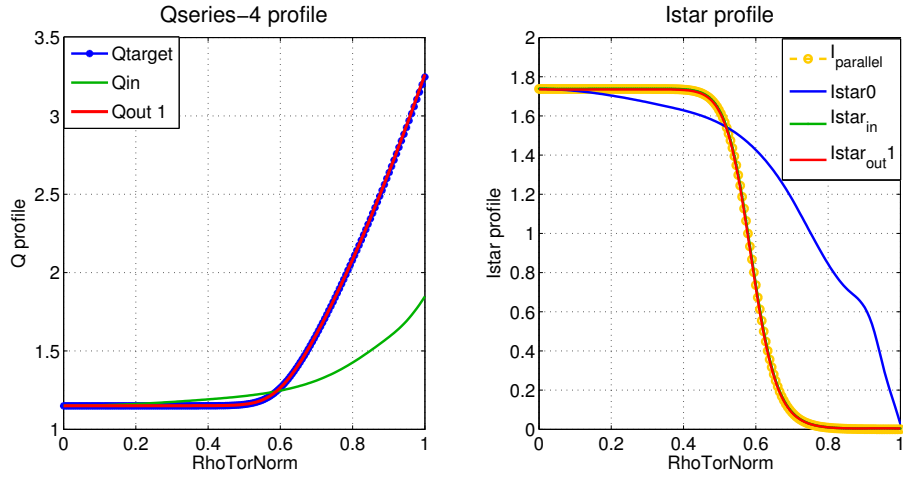
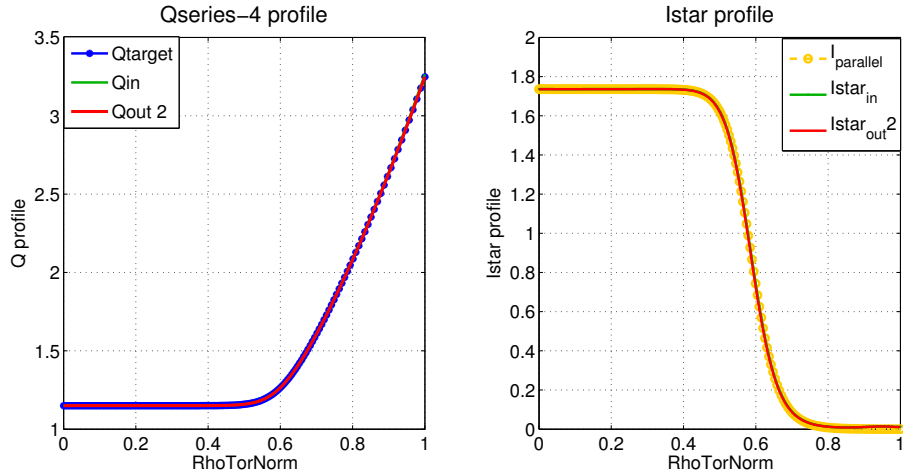
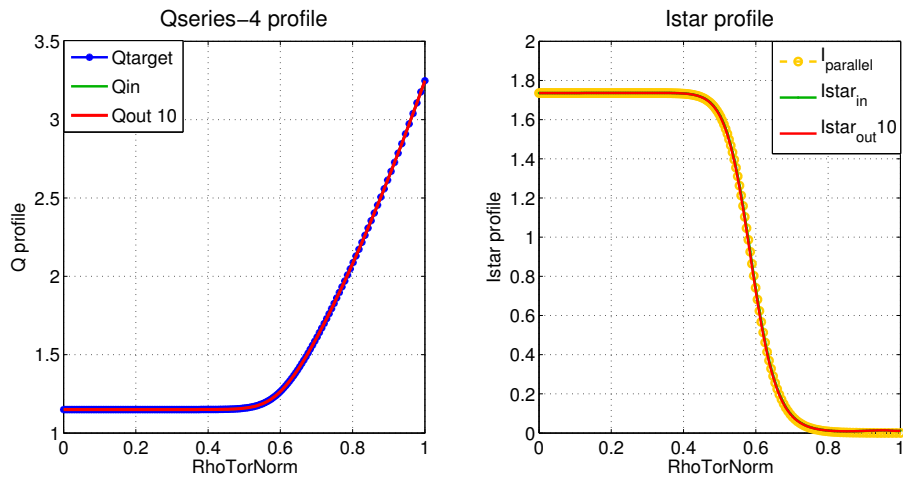
(a) Fourth q -series profile. Run 1.(b) Fourth q -series profile. Run 2.(c) Fourth q -series profile. Run 10.

Figure 12: Fourth q -series profile. Run 1 to 10 using I^* input expression (50), $\text{NFUNRHO}=1$, $\alpha = 1$. From the first run the output safety factor is very well superimposed to the target one and this convergence holds over the runs. The first computation of I^* using formula (50) already corresponds to the expected I_{\parallel} and so does the output profile.

3.4.3 Test case with a specified profile

A question about CHEASE from a SPC PhD student has revealed to be a very good test for the method developed above. The question was about varying the pressure profile while keeping the same safety factor. The original EXPEQ file with the plasma shape and the pressure and current profiles are shown on the left graph in figure 13. The aim is then to keep the same safety factor profile while lowering the pressure profile from the blue curve to the green one of the right graph in figure 13. A first run with the received EXPEQ file (figure 13) was performed with CHEASEgui and its output EXPEQ file (figure 14) was then used in input of our method. This was done mainly to avoid a divergence in the calculation which appeared when using NPPFUN=8 (corresponds to input p) and disappeared when using NPPFUN=4 (corresponds to input p'). The runs have been made with $\alpha = 0.5$ as it leads to a better convergence of the safety factor profile at the edge. With $\alpha = 1$, the output profile was oscillating between above and below the targeted profile over the runs and reducing the α value helped solving that problem. As the given profile of I^* was very abrupt at the edge, the last point of the targeted safety factor profile was lowered to avoid a discontinuity in the profile. One can see in figures 15 that the I^* tends to stabilize itself at the edge over the runs. For this specific profile, the use of the α led to a real improvement and will be necessary too for the implementation in CHEASE, as detailed later on.

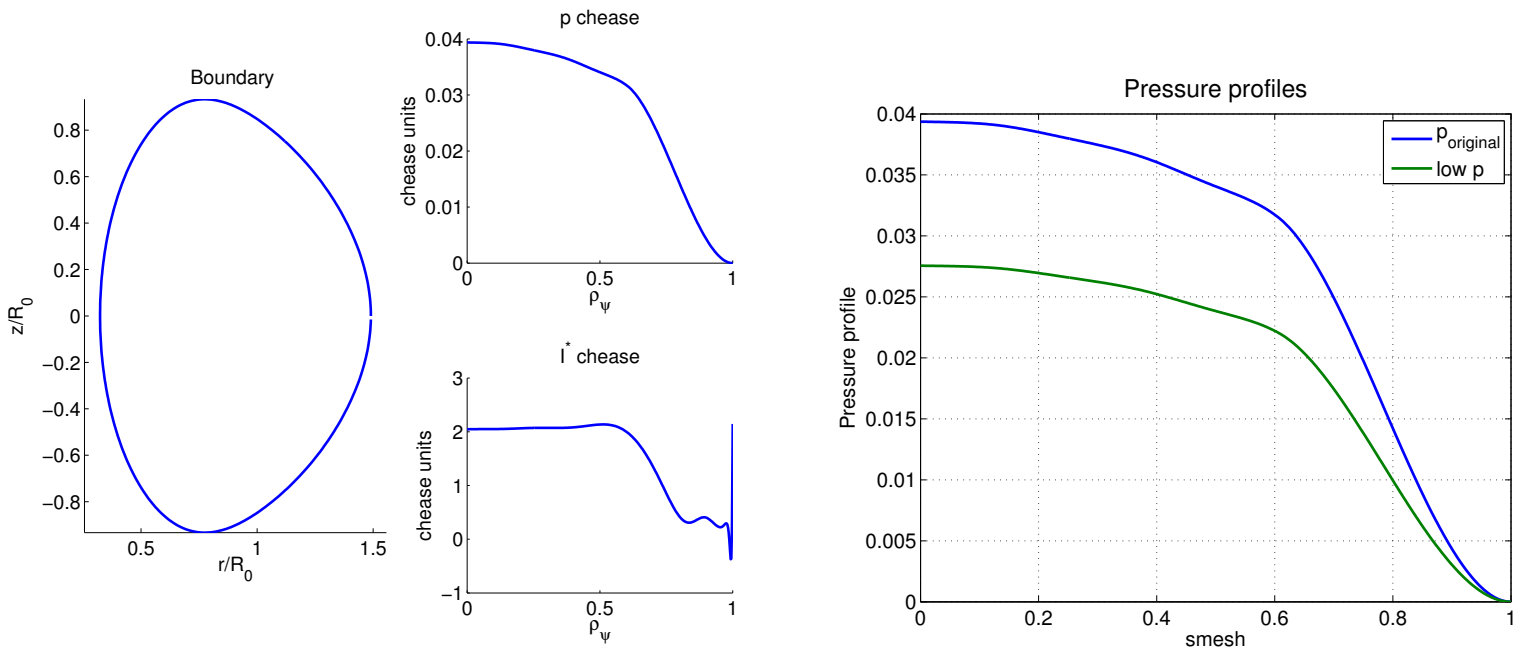


Figure 13: Left figure shows the original EXPEQ file (with p as input) received while the right figure presents the original pressure profile (blue curve) and the lowered one (green curve): $p_{low} = 0.7 \cdot p_{original}$

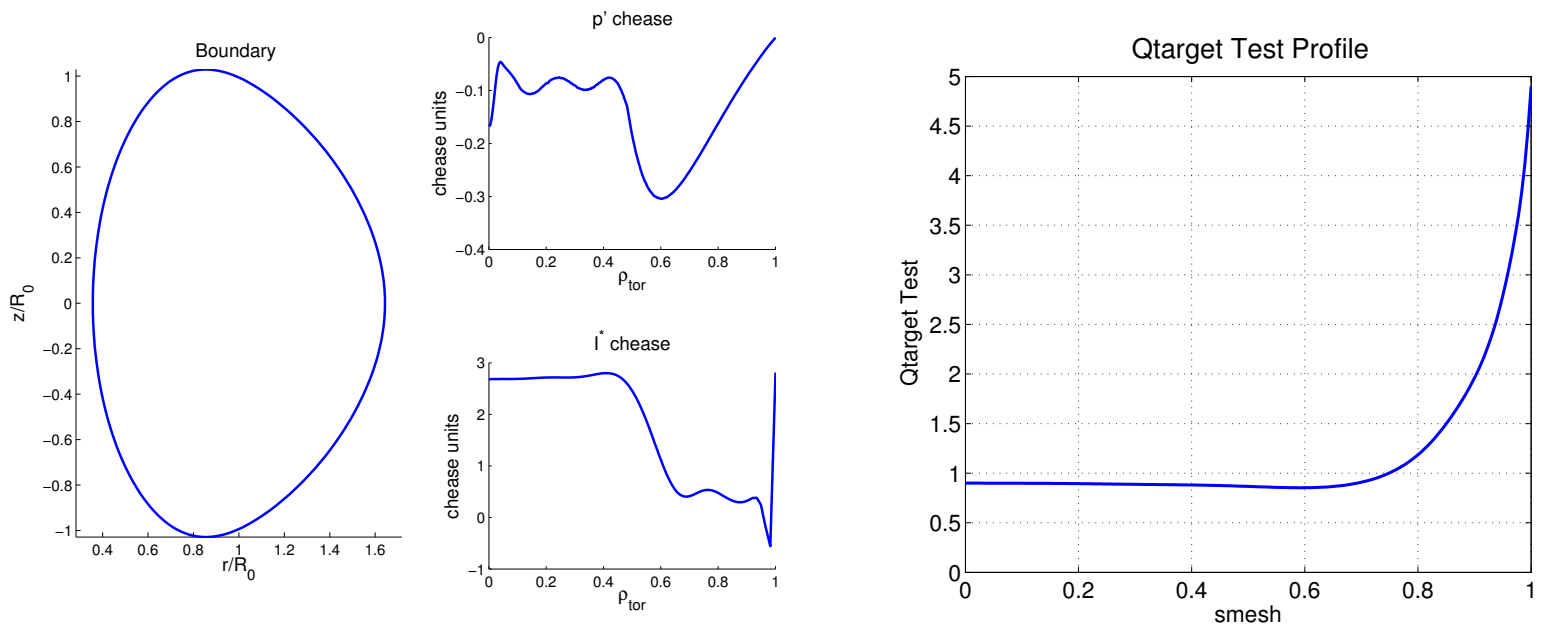
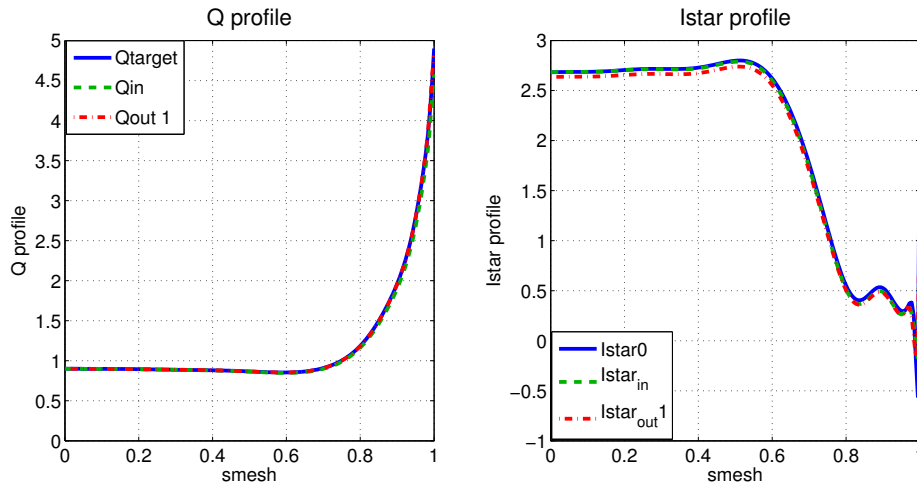


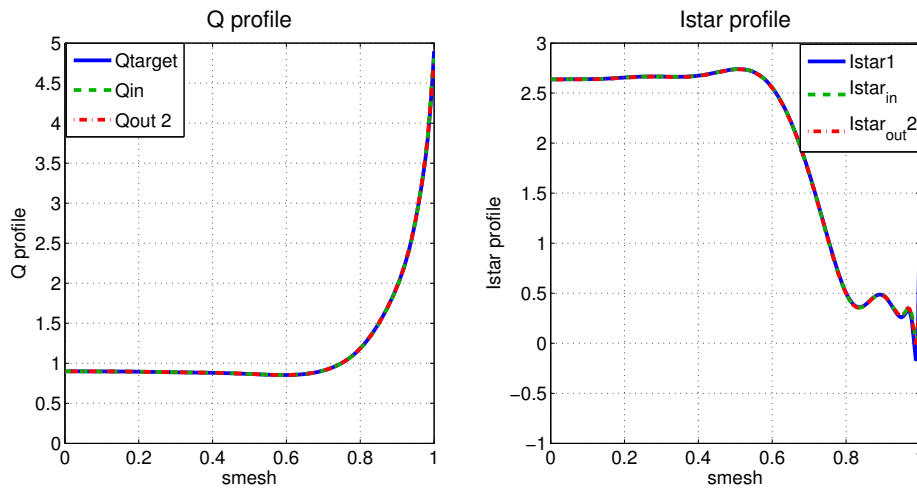
Figure 14: Left figure shows the input EXPEQ file (with p') used for the external runs of CHEASE while the right figure presents the targeted safety factor profile (the one obtained in output of CHEASEgui with input 13 EXPEQ file).

3 USING A PREDEFINED Q PROFILE AS CHEASE INPUT WITH AN EXTERNAL LOOP TO FIND THE APPROPRIATE I^* AND TT' EXPRESSIONS

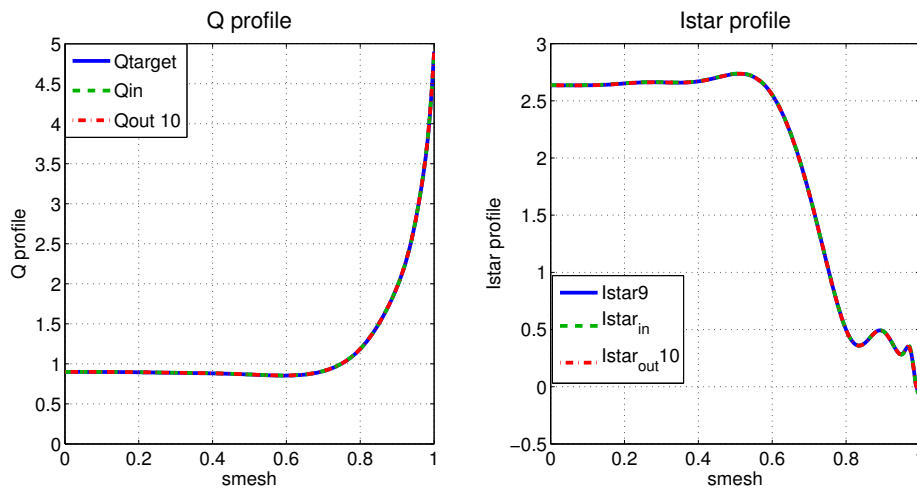
Safety factor profile as CHEASE input



(a) Test case. Run 1 with $\alpha = 0.5$.



(b) Test case. Run 2 with $\alpha = 0.5$.



(c) Test case. Run 10 with $\alpha = 0.5$.

Figure 15: Input I^* , NSTTP=2, NFUNRHO=0, $\alpha = 0.5$. Q and I^* profiles after a few runs of CHEASE using input I^* formula (50). The graphs show that the solution is steadily converging and leads to very good results.

4 Implementing the procedure into CHEASE

Now that the expression (50) giving the surface averaged current density as a function of the safety factor has been verified successfully with several safety factor profiles in the previous section, the true purpose of this work can now be addressed, namely to implement this expression directly into the CHEASE code.

4.1 Approach

As introduced above, in order to be able to specify the safety factor q as input, a new NSTTP case has to be implemented. Until now, the following options were available:

- case NSTTP = 1 $\rightarrow p'$ and TT' as inputs
- case NSTTP = 2 $\rightarrow p'$ and I^* as inputs
- case NSTTP = 3 $\rightarrow p'$ and I_{\parallel} as inputs
- case NSTTP = 4 $\rightarrow p'$ and $J_{\parallel} = \frac{\langle \mathbf{j} \cdot \mathbf{B} \rangle}{B_0}$ as inputs

Note that while it is more common to use p' as first entry profile one can rather provide the pressure profile and run CHEASE with NPPFUN=8 instead of NPPFUN=4. As a reminder, the purpose is to implement two alternative options where the safety factor can be given as input and then get imposed internally via the current density profile expression $I^*(q)$ or via $TT'(q)$ to solve the Grad-Shafranov equation:

- case NSTTP = 5 $\rightarrow p'$ and q as inputs \rightarrow internal computation of $I^*(q)$
- case NSTTP = 6 $\rightarrow p'$ and q as inputs \rightarrow internal computation of $TT'(q)$

However, remembering the results presented in section 3.2, when one tries to impose the safety factor directly through TT' using its expression:

$$T = 2\pi \frac{q}{C_2}$$

the results were not conclusive and the output was diverging, mainly because of the derivative term in T' . This indicates that the case NSTTP=6 will in fact not be a conceivable option and will be left behind from here on.

The NSTTP = 5 line of calculation should be similar to the case NSTTP = 2 except that the input profile, stored in the variable RFUN in the code will be q instead of I^* . The averaged current density profile will then be computed internally from this profile with expression (50). Hence, in some subroutines, the condition "*if NSTTP = 2*" has been updated to "*if NSTTP = 2 or NSTTP = 5*".

To elaborate this alternative, one had to add the computation of the C_3 surface

integral in order to be able to compute the surface average of the poloidal magnetic field:

$$\langle B_p^2 \rangle = \frac{\oint_{s=const} \left(\frac{|\nabla\psi|}{R} \right)^2 J d\chi}{\oint_{s=const} J d\chi} = \frac{C_3}{C_1} \quad (55)$$

The surface coefficients (expression (13)) are computed in subroutine CINT. For memory optimization purposes, once each coefficient has been computed separately, only the required ratios are stored into the variables. Even though for NSTTP = 5 one needs to compute C_3 (which was before only needed for cases NSTTP = 3 or 4), one also needs to keep the same ratios in the same variables as for NSTTP = 2 to be consistent with further calculations. Therefore for NSTTP = 5, one can now make use of the following coefficients (CID0 & CID2 remaining the same as for NSTTP = 2):

$$\begin{cases} CID0 = \frac{CID0}{CIDQ} \rightarrow \frac{C_0}{C_2} \\ CID2 = \frac{CIDR}{CIDQ} \rightarrow \frac{C_1}{C_2} \\ CID3 = \frac{CID3}{CIDR} \rightarrow \frac{C_3}{C_1} \end{cases} \quad (56)$$

The main focus has been to compute the proper I^* profile (expression (50)) from the safety factor's input. This calculation was first implemented into subroutine PRFUNC which aims to compute the second input profile. However, as can be understood by looking at figure 17 which attempts to summarize in a sketch the procedure followed by CHEASE, subroutine PRFUNC usually interpolates the I^* profile from constant-flux surfaces to CHEASE surfaces. But here the I^* was systematically re-calculated instead of being kept fixed on flux-surfaces until a new solution ψ was computed. The I^* profile is now computed on flux-surfaces in ISOFUN and is interpolated on CHEASE's surfaces in PRFUNC.

The architecture of the algorithm in CHEASE is the following, with two successive sets of iterations: a first one on a coarse grid (NS=NT=24 & NISO=100) and a second one on a more precise grid (for example with NS=NT=40 & NISO=180 but these values can be adjusted by the user). A first guess-solution is chosen in subroutine GUESS from a paraboloid flux profile in order to initiate the iteration, the NISO constant-flux surfaces are then computed in subroutine ISOFIND in terms of the equilibrium coordinates (σ, θ) . The surface integrals C_i can then be calculated on these surfaces, in subroutine CINT, before being used in subroutine ISOFUN to compute the I^* profile for the case NSTTP = 5 (precise steps of computation are listed below). The profiles TT' and p' are also evaluated on flux-surfaces in this subroutine which allows to describe the current density j_ϕ . The source term j_ϕ is then computed on CHEASE mesh by subroutine CURENT (with back and forth calls to PRFUNC required to interpolate the I^* profile on CHEASE surfaces) with surface integrals C_i being kept constant. This step consists in fact of computing the current density value for each point of the CHEASE mesh. Knowing all the values $j_\phi(\sigma_i, \theta_j)$

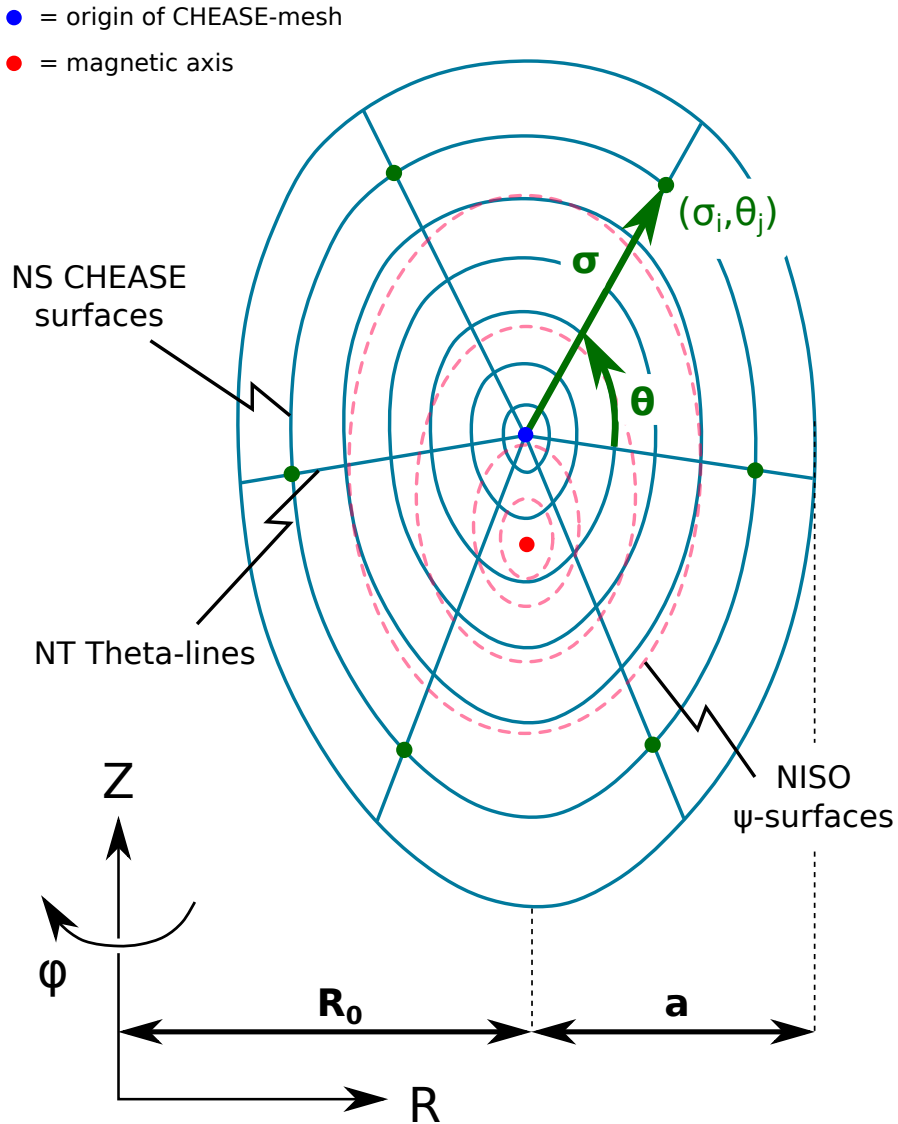


Figure 16: Constant- ψ surfaces are represented in 1D by the dashed pink lines in this figure surrounding the magnetic axis (R_{mag}, Z_{mag}). They are not to be mistaken for the CHEASE surfaces, represented in 1D by the blue lines, which illustrate the CHEASE mesh (σ_i, θ_j) on which the Grad-Shafranov equation is solved in the code. They start from the origin of CHEASE mesh (R_C, Z_C) (which can be less-centred than drawn on the figure) and are homotheties of the plasma boundary. The aim of the numerical iteration over the current density profile is to find the magnetic axis and to compute an output solution centred on it.

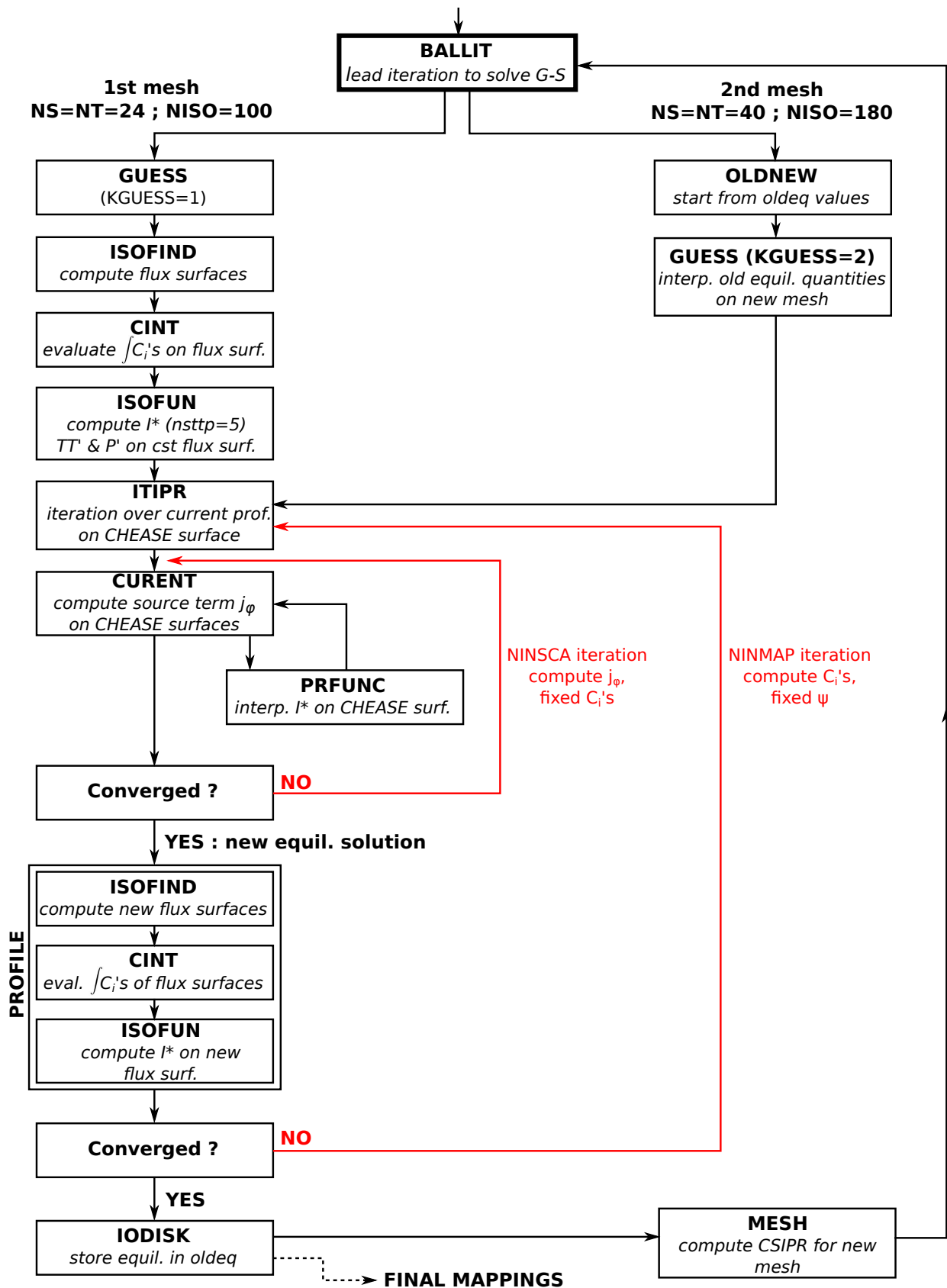


Figure 17: Sketch of the flow diagram in CHEASE.

(figure 16), the current density profile is then computed by 2D-Gauss-integrations in subroutine NONLIN.

Notice that, on figure 16, when going from a flux-surface to a CHEASE surface, the variation of ψ is so small that the interpolated I^* profile in subroutine PRFUNC is nearly constant.

Once the equilibrium solver has converged to give a new $\psi(\sigma_i, \theta_j)$ solution, which stands as the new equilibrium profile, one tries to find the surfaces $\psi = \text{constant}$ (with *constant* being a 1D array) in ISOFIND. The surface integrals C_i are then re-evaluated. This outer loop over ψ only stops once the equilibrium quantities do not vary much from one ψ solution to the next one. This is evaluated with the RESIDUE OVER MAPPING quantity which should become smaller than a predefined number ϵ . These convergence properties are explained in details in paper [2] *The CHEASE code for toroidal MHD equilibria*.

The equilibrium solution on this first mesh is then stored in subroutine IODISK in order to start the second set of iterations by interpolating these quantities on the new, more precise mesh. The same steps are then followed as before which solve the Grad-Shafranov equation with two nested Picard iterations visible in figure 17. Once convergence is achieved, a final mapping of the equilibrium quantities is performed into the flux coordinate system (ψ, χ, Φ) (cf section 3 of paper [2]).

CHEASE can generate a whole variety of solutions to the Grad-Shafranov equation:

$$\tilde{\psi}(R, Z) = \lambda\psi(R, Z) + \psi_0 \quad (57)$$

which are all solutions of a rescaled Grad-Shafranov equation:

$$\Delta^* \tilde{\psi} = \lambda \Delta^* \psi \quad (58)$$

The solution given in output is computed with respect to the boundary conditions specified by the user. They are usually given for the safety factor profile values at the center or at the edge which determines the value for λ and rescales the solution in subroutine NOREPT.

The main steps performed in subroutine ISOFUN to compute the I^* expression (50) are listed below:

1. Interpolate input safety factor profile stored in RFUN(1:NPPF) from input mesh FCSM(1:NPPF) on mesh CSIPR(1:NISO) (ρ_{pol} mesh used for the calculation) in variable Qtarget(1:NISO) with function INTERPOS.
2. Compute X1 and X2 on the NISO flux surfaces:

$$X1(i) = CID3(i)*TMF(i)*CIDQ(i)/(2*pi)$$

$$X2(i) = (2*pi*CIDR(i))*X1(i)/QtargEtarget(i)$$

3. Compute derivative dX2dpsi(1:NISO) with function INTERPOS.
4. Set value for α and compute I^* expression (50) on flux surfaces:

$$\begin{aligned} \text{IstarTarget}(i) &= (1-\alpha)*\text{IstarTarget}(i) \\ &+ \alpha*(CID2(i)/CID0(i))*dX2dpsi(i)/(2*pi*CIDR(i)) \end{aligned}$$

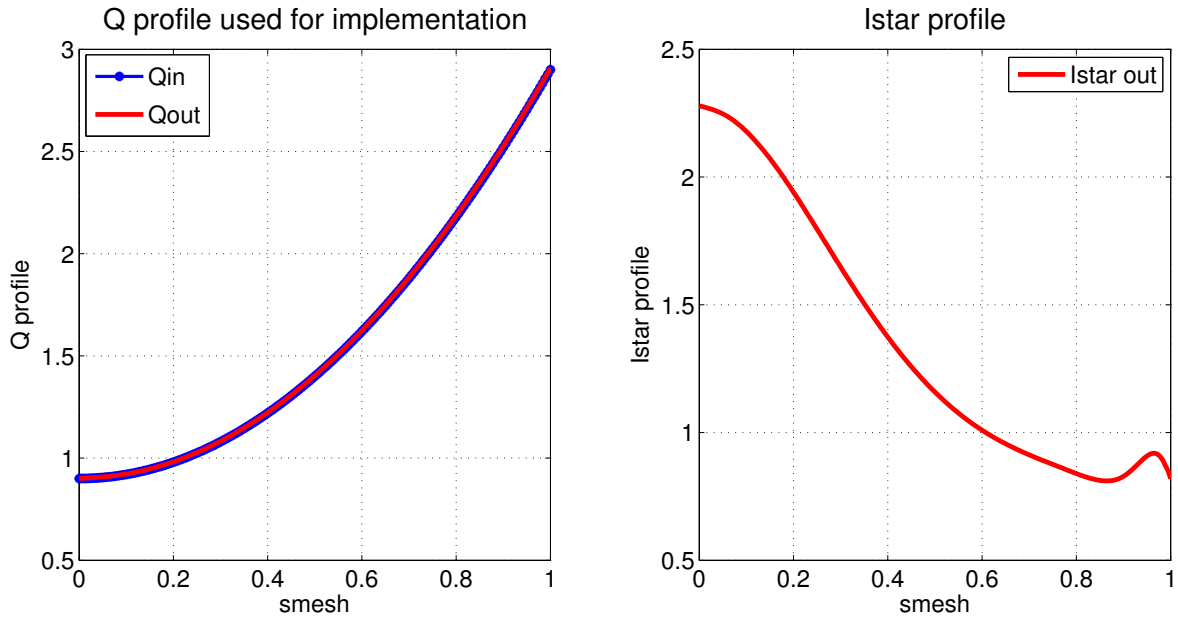


Figure 18: Targeted safety factor profile (blue curve) while testing ways of implementing the case $NSTTP=5$ internally. Once run properly, CHEASE provided an output safety factor (red curve on the left graph) corresponding exactly to the input profile. The output corresponding I^* profile is reported in red on the right graph.

One has to be careful when using the mesh. CSIPRI indicates the beginning of each interval in the code while CSIPR stands for the center of the corresponding interval. PSIISO, which is computed from CSIPR is also located at mid-intervals, except for the last iteration in CHEASE where it is shifted so as to indicate the beginning of the interval. This can generate a last value gap between CSIPR (global variable) and ZS (local variable computed from PSIISO) and could lead to an offline last value for the output safety factor profile with respect to the target profile.

Even though CHEASE now succeeds into providing a fully-consistent output equilibrium with an input safety profile, one has to point out that the computation of equilibria is a lot slower than for $NSTTP=2$. Even since the introduction of the α variable which makes computation much faster, they remain slow compared to the case $NSTTP=2$.

Now that one is able to specify a safety factor profile as input, the functions to read and plot the EXPEQ file, so as the CHEASEgui interface have been updated with the new $NSTTP=5$ case. An illustration of PLOT_EXPEQ with an input safety factor profile can be seen in figure 19.

4.2 Validation with the q profiles tested externally

Now that CHEASE manages to run with the option $NSTTP = 5$ (input EXPEQ 19) and leads to the very same output safety factor profile as the one given in input (figure 18), the implemented method will be tested with the same profiles which

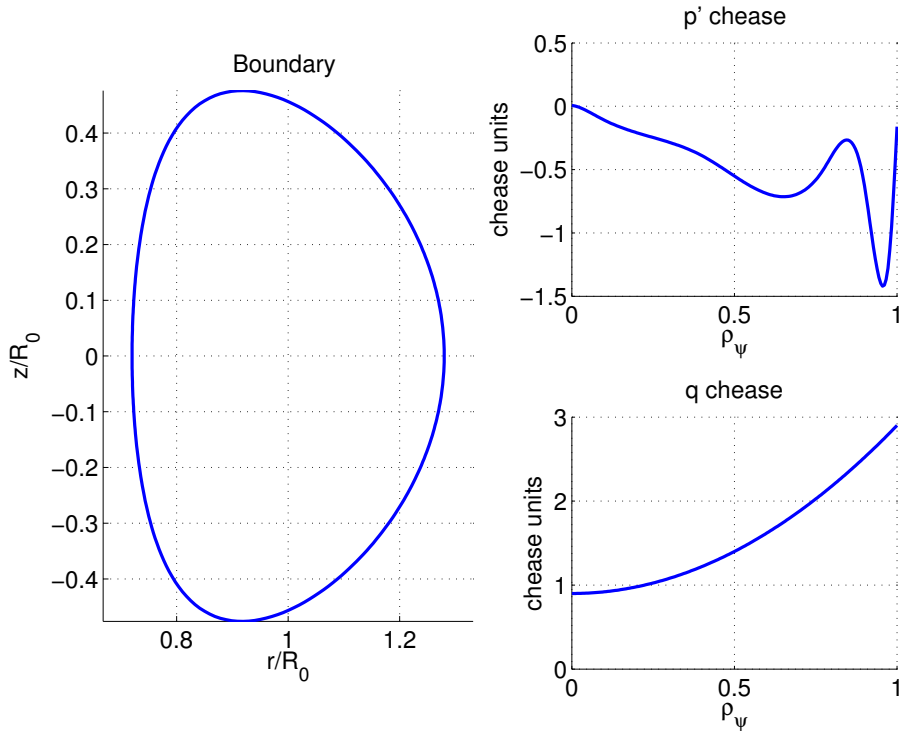


Figure 19: *Just one example to illustrate the fact that the safety factor profile can now be given as input in the EXPEQ file.*

have been used externally in section 3.4.

4.2.1 First profile

The results obtained with the first safety factor profile received as input are shown in figure 20. The input safety factor profile is represented by the blue curve while the output safety factor profile is represented by the red one on the left graph of this figure. The fact that the two curves are perfectly superimposed and that the other output quantities, especially the averaged current density profile I^* are consistent, confirms the success of the implemented calculation.

4.2.2 Series of four profiles

The respective results for the four input q -series profiles are presented in figures 21, 22, 23 and 24. The very same conclusion as the one made for the previous profile applies here and contributes in validating the implemented method.

4.2.3 Test case with a specified profile

The convergence of the test safety factor profile sent by the SPC PhD student has been more challenging to achieve. Indeed, as it had already been noticed while iterating externally, the edge slopes of q and I^* were very abrupt and the output safety factor profiles kept oscillating between above and below the targeted edge

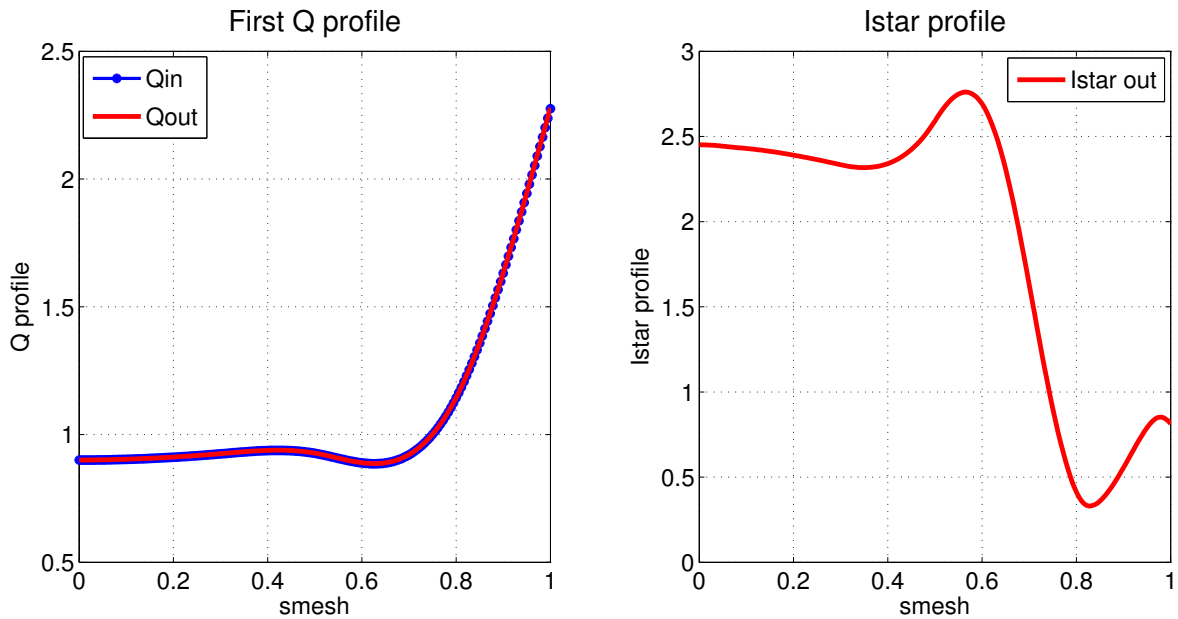


Figure 20: *First safety factor profile. Left figure shows input q-profile in blue and output profile in red. With these two curves perfectly superimposed and a credible output averaged current density profile (right figure), the numerical method is validated for this profile.*

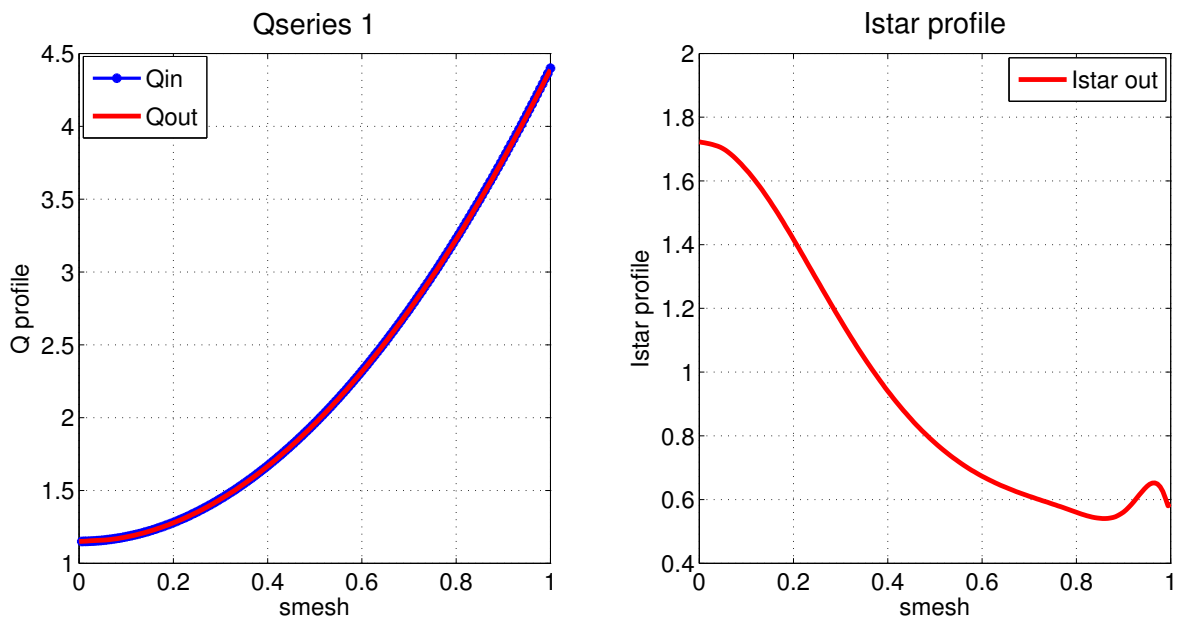


Figure 21: *First q-series profile. Left figure shows input q-profile in blue and output profile in red. With these two curves perfectly superimposed and a credible output averaged current density profile (right figure), the numerical method is validated for this profile.*

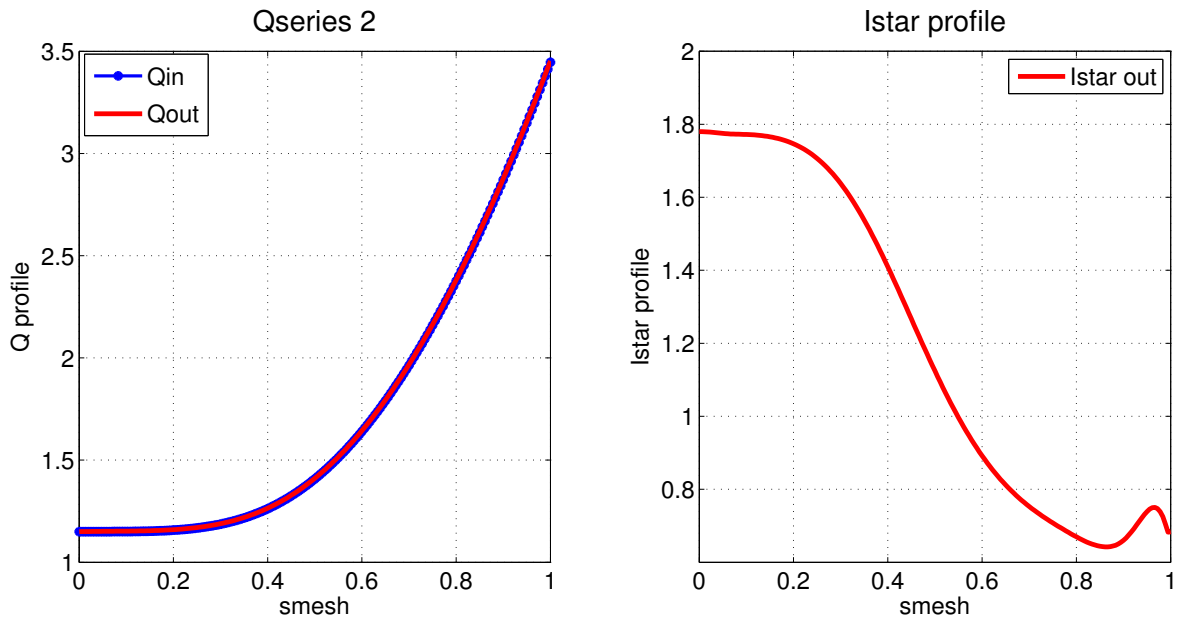


Figure 22: *Second q -series profile. Left figure shows input q -profile in blue and output profile in red. With these two curves perfectly superimposed and a credible output averaged current density profile (right figure), the numerical method is validated for this profile.*

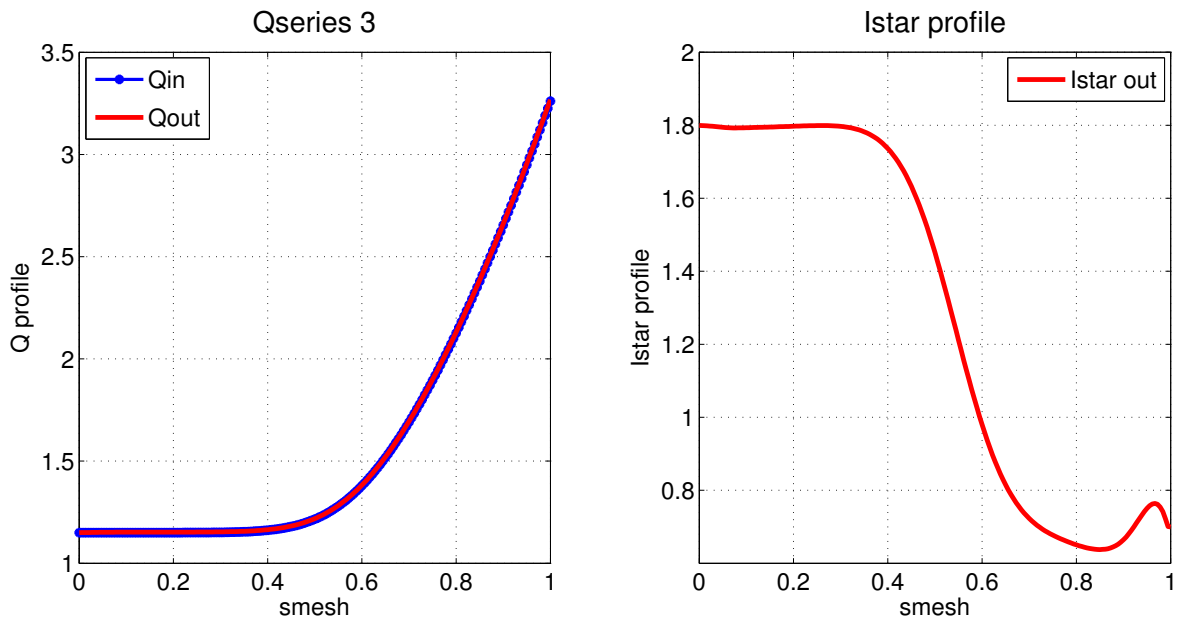


Figure 23: *Third q -series profile. Left figure shows input q -profile in blue and output profile in red. With these two curves perfectly superimposed and a credible output averaged current density profile (right figure), the numerical method is validated for this profile.*

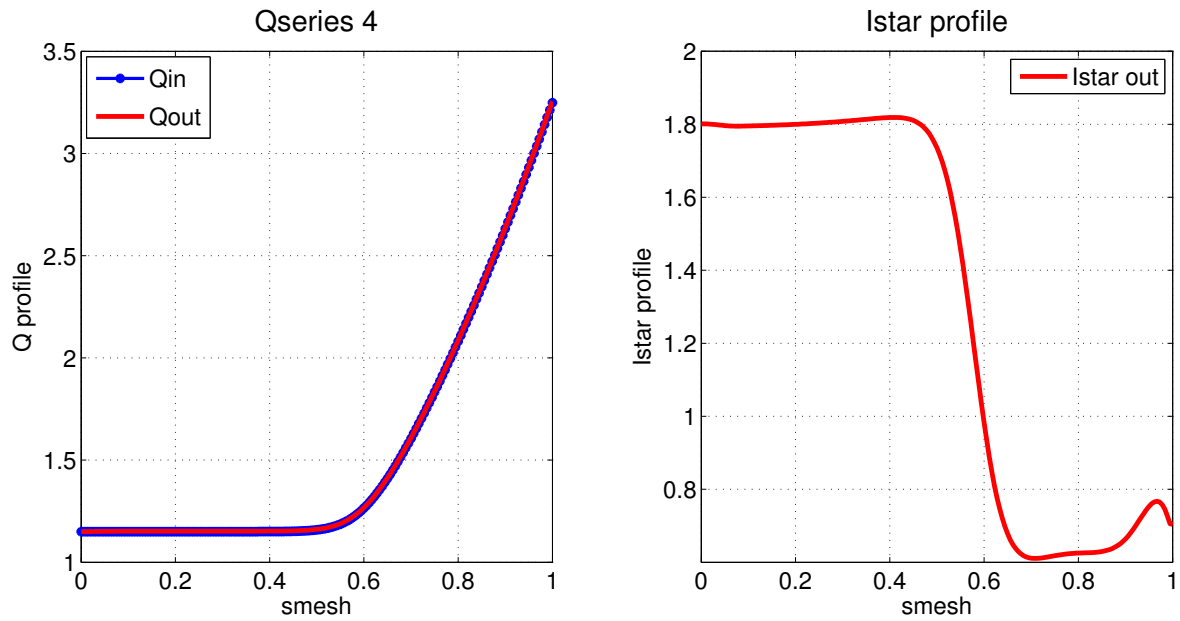


Figure 24: *Fourth q-series profile. Left figure shows input q-profile in blue and output profile in red. With these two curves perfectly superimposed and a credible output averaged current density profile (right figure), the numerical method is validated for this profile.*

value until the introduction of α . The same method has been applied internally and solved the problem, reducing significantly the iteration's time along the way.

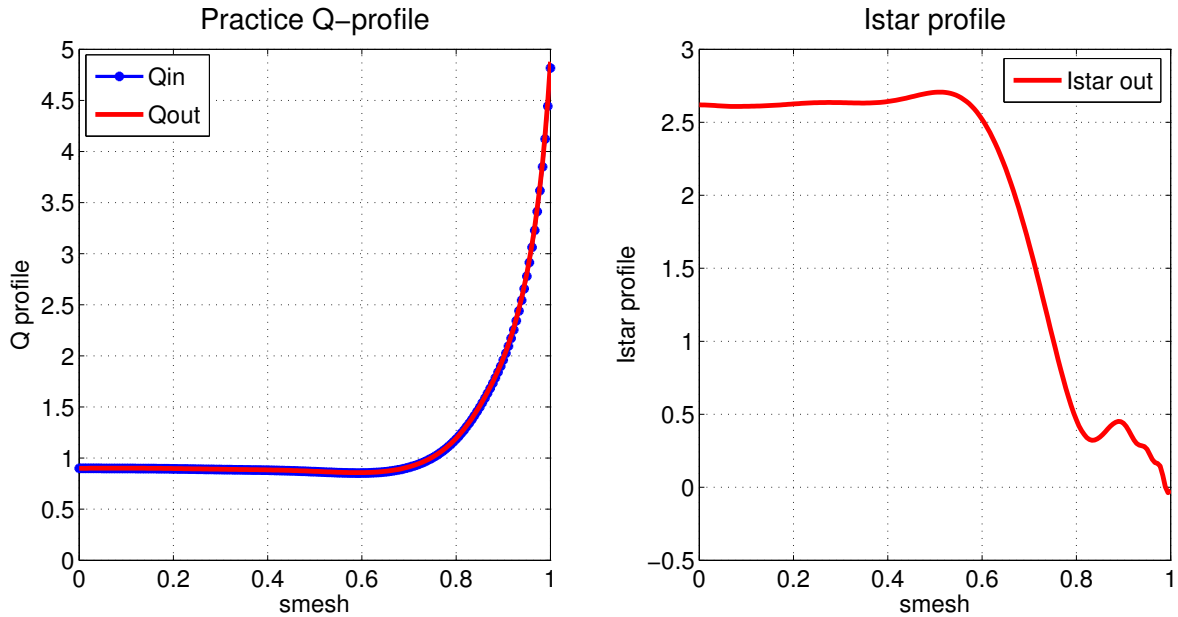


Figure 25: *Test case q-profile. Left figure shows input q-profile in blue and output profile in red. With these two curves perfectly superimposed and a credible output averaged current density profile (right figure), the numerical method is validated for this profile.*

5 Applying the procedure for tearing modes stability analysis

Tearing instabilities can occur when field lines break and reconnect in the plasma. The reconnection can only occur at locations with rational values of the safety factor and in the presence of resistivity (that is to say that one has to assume there is some localised resistivity on a tiny surface where reconnection could happen while the ideal MHD holds everywhere else). When experiencing a radial perturbation two separate magnetic field lines next to each other can connect. This disrupts completely the plasma stability as this new closed field line layer creates a magnetic island which changes the pressure profile (same value for the pressure everywhere inside the island) by creating a flat plateau where reconnection occurred. The safety factor profile can indicate whether or not an equilibrium is stable or unstable by evaluating if a perturbation would tend to grow or disappear. Slightly modifying the q -profile could make perturbations to evolve in a different way. The following section is meant to focus on this influence.

Starting from a given safety factor, one will then modify this profile around one of the rational values $2/1$ or $3/2$ (as they are known to be the most likely to generate magnetic reconnection). To know if the plasma is stable or not around this value of q one has to evaluate the quantity Δ' (expression (59), from book *Tokamaks* [7]): if it is positive, this means that the configuration is unstable and reconnection occurs but if it turns out to be negative, this means that the configuration is stable. Indeed, as the amplitude of the instability is exponentially-dependent on Δ' , a positive

value would make it grow exponentially while a negative value would make it vanish quickly.

$$\Delta' = \frac{1}{B_r(r_s)} \left[\frac{dB_r}{dr} \right]_{r_s-\epsilon}^{r_s+\epsilon} \quad \epsilon \rightarrow 0 \quad (59)$$

where B_r is the perturbed radial magnetic field and r_s denotes the resonant surface $r = r_s$ where $m = nq$. Practically, one uses the file EQDSK.OUT generated by CHEASE when given in input the safety factor profile and run the routine DELTAP-CYL with it. This directly computes the values of $r_s \Delta'$.

From the different safety factor profiles studied in the previous section, the one referred to as the "first profile" (figure 20) happens to be stable for both modes 2/1 and 3/2 with respective $r_s \Delta'$ -values of $(-1.4801 \cdot 10^1)$ and (-2.5004) . The 3/2-modified profile (with $\frac{dq}{d\rho}|_{q=3/2} = 0$) represented by the red curve in figure 26a leads to:

$$\begin{cases} q = 2/1 \rightarrow r_s \Delta' = -2.52383 \cdot 10^1 \\ q = 3/2 \rightarrow r_s \Delta' = 5.21293 \cdot 10^2 \end{cases} \quad (60)$$

while another 3/2-modification of the profile (with $\frac{dq}{d\rho}|_{q=3/2} = 10$), drawn in red on figure 26b, leads to:

$$\begin{cases} q = 2/1 \rightarrow r_s \Delta' = 8.76578 \\ q = 3/2 \rightarrow r_s \Delta' = 6.5870 \cdot 10^1 \end{cases} \quad (61)$$

The first modification (figure 26a) therefore tends, roughly speaking, to stabilize mode 2/1 and to destabilize mode 3/2 while the second modification (figure 26b) tends to destabilize both modes.

Starting this time from an unstable mode, one can look at the 2/1-mode of the third q-series profile (figure 23) for which:

$$\begin{cases} q = 2/1 \rightarrow r_s \Delta' = 2.93169 \cdot 10^{-1} \\ q = 3/2 \rightarrow r_s \Delta' = 4.5149 \end{cases} \quad (62)$$

and apply the same modifications as for the previous profile but this time near the 2/1 mode. The first 2/1-modified profile (with $\frac{dq}{d\rho}|_{q=2/1} = 0$) represented by the red curve in figure 27a leads to:

$$\begin{cases} q = 2/1 \rightarrow r_s \Delta' = 1.68557 \cdot 10^3 \\ q = 3/2 \rightarrow r_s \Delta' = 4.89832 \end{cases} \quad (63)$$

The second 2/1-modified profile (with $\frac{dq}{d\rho}|_{q=2/1} = 10$) represented by the red curve in figure 27b leads to:

$$\begin{cases} q = 2/1 \rightarrow r_s \Delta' = 1.03947 \cdot 10^2 \\ q = 3/2 \rightarrow r_s \Delta' = 4.14678 \end{cases} \quad (64)$$

Both modifications therefore strongly destabilize the 2/1-mode while having no-effect on the 3/2-mode.

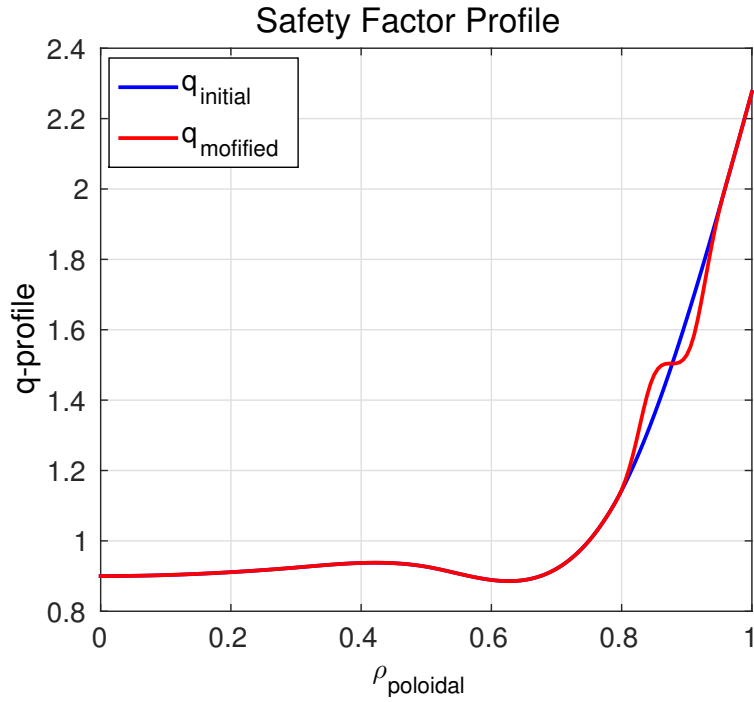
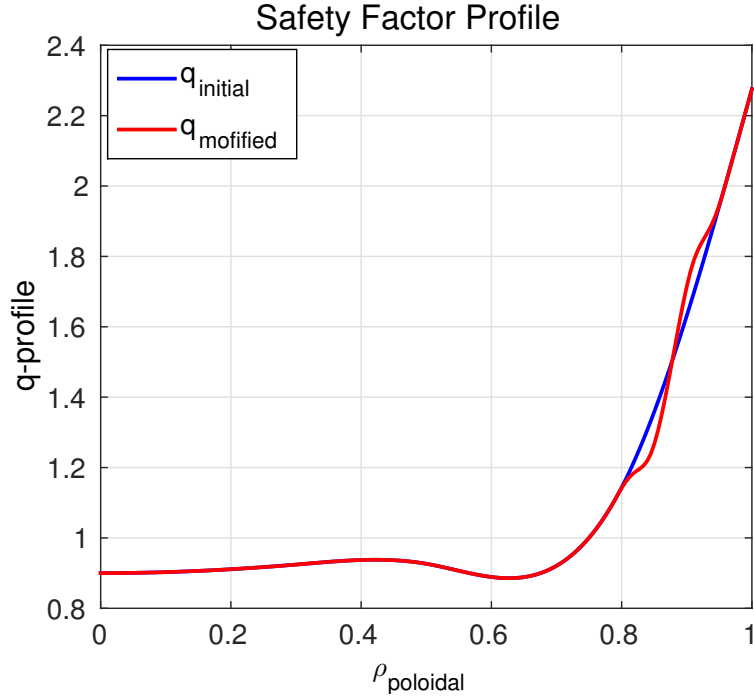
These effects of the safety factor profile on equilibrium stability would require to be studied in more details with different specified profiles in order to be able to deduce some results. Nevertheless, this section opens the way to a new range of equilibrium-dependence studies. Indeed, the previous values confirm that the safety factor profile has a great impact on the equilibrium stability and that fine-tuning it can be crucial to guarantee stability with respect to tearing modes.

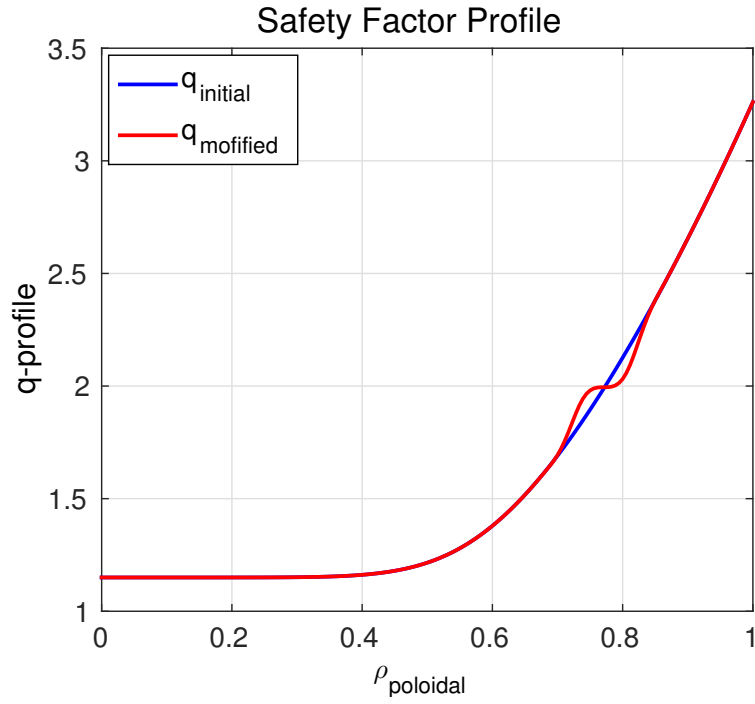
6 Conclusion

This work was developed within a master project which main purpose was to develop a method enabling the user to specify a safety factor profile as input of the equilibrium solver CHEASE. Two different alternatives were explored in order to impose the safety factor profile either via the averaged current density $I^*(q)$ or via $TT'(q)$. Prior to implementing the proper method in the core code, tests were conducted with an external computation of both $I^*(q_{target})$ and $TT'(q_{target})$ as input profiles for CHEASE. No $TT'(q)$ expression has demonstrated good-convergence properties but a suitable expression for $I^*(q)$ has been constructed, Eq. (50), and tested with several safety factor profiles, leading each time to a fully consistent equilibrium. Only one method has then been implemented into CHEASE, referred to as the NSTTP=5 case. This method consists of giving q as input and internally computing the $I^*(q)$ expression which was demonstrated to be successful externally. This calculation, implemented into the subroutine ISOFUN, has confirmed very good convergence properties for several tested safety factor profiles without any continuity issue in the solution. This extension of CHEASE was then used to study the influence the safety factor profile could have on tearing instabilities. This was confirmed to be crucial and would require further investigations. Being now able to specify the safety factor profile as CHEASE input opens the way to further equilibrium stability studies as the whole output equilibrium of CHEASE could respond differently to induced perturbations depending on the input q profile. Note that an extension to this new NSTTP=5 case is available, manually at this stage, which consists of modifying slightly the edge q derivative in order to obtain $I^* = 0$ at the edge, since I^* depends on $dq/d\psi$ as seen in Eq. (50). Using CHEASE functionalities, it is easy to use the resulting I^* profile and modify it slightly near the edge as well, since with our method we do not obtain unphysical edge current.

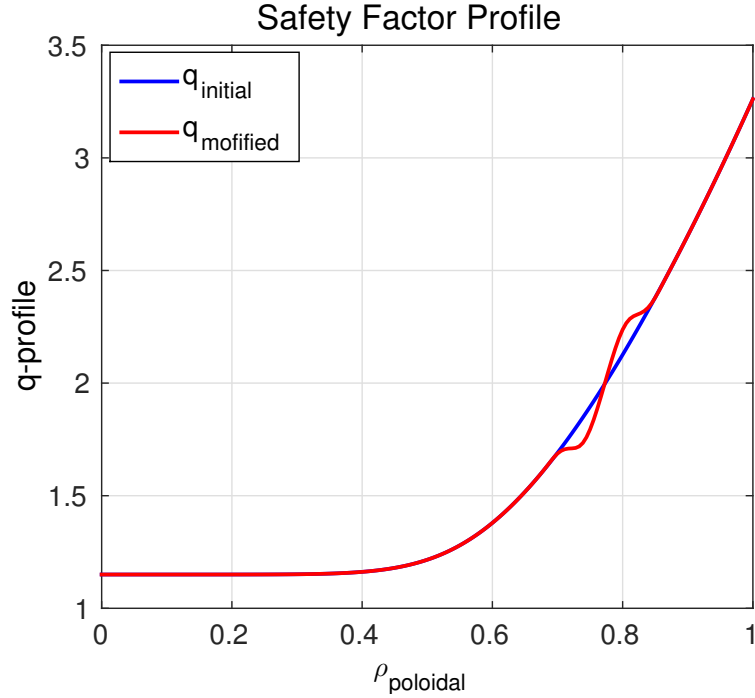
7 Acknowledgements

This work was supported in part by the Swiss National Science Foundation. It was mainly developed during L. Blondel master project and integrated into the main CHEASE svn/trunk project (<http://spc.epfl.ch/chease>).

(a) Modified "first" q -profile with a 0-derivative at $q = 3/2$.(b) Modified "first" q -profile with a derivative equal to 10 at $q = 3/2$.Figure 26: First studied q -profile modified near surface where $q = 3/2$ with a degree three polynomial and a derivative equal once to 0 and once to 10 at $q = 3/2$.



(a) Modified *Qseries-3* profile with a 0-derivative at $q = 2/1$.



(b) Modified *Qseries-3* profile with a derivative equal to 10 at $q = 2/1$.

Figure 27: *Third Q-series profile modified near surface where $q = 2/1$ with a degree three polynomial and a derivative equal once to 0 and once to 10 at $q = 2/1$.*

Appendices

A Selecting the updated quantity

Remembering figure 1 showing the current density curve obtained from updated equation (15), there is a real need to limit the correction induced in the I^* curve by the new safety factor profile. A first attempt, presented in this appendix, was then to update either the q term or the derivative term $\frac{d}{d\psi} \left[\frac{q}{C_2} \right]$ but no longer both at the same time.

Update only q

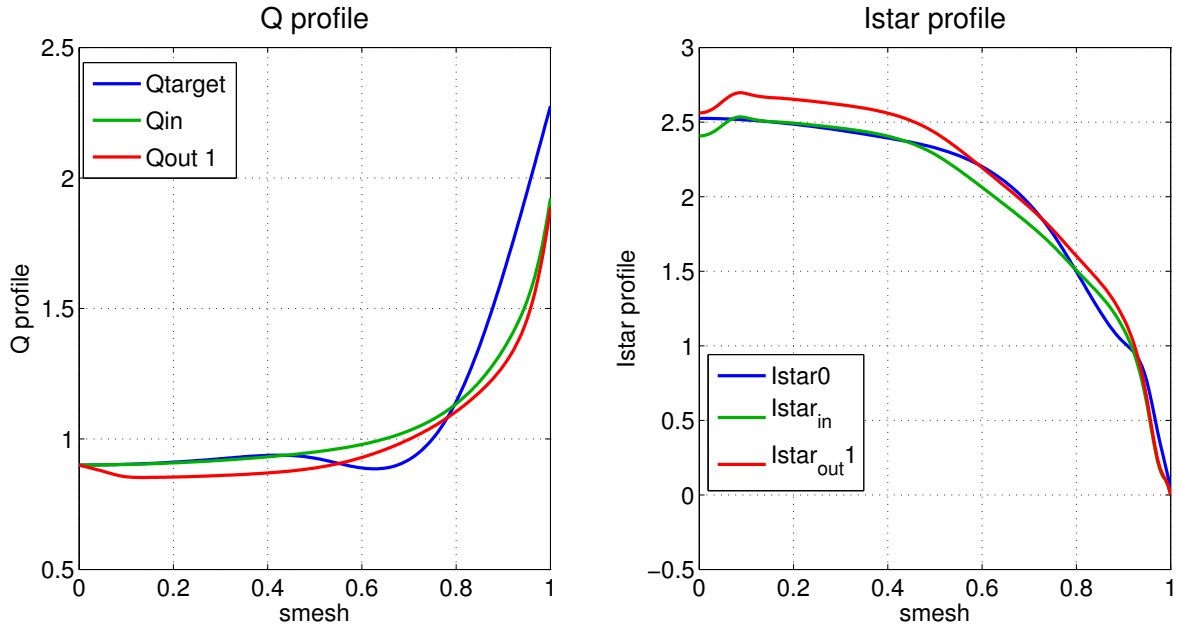
The results are presented in figures 28. At least, with only an update of the q term, CHEASE manages to run, as we can see the I^* input profile is a lot less chaotic than before. The two runs presented in figures 28 have been done with a boundary condition, added with the *interpos* tool when calculating the derivative $\frac{d}{d\psi} \left(\frac{q}{C_2} \right)$, imposing $I^*(edge) = 0$. Without this condition the results were far worse and the safety factor profile obtained in output of the first run was a lot below the targeted one. However, even if CHEASE manages to run, the profiles become chaotic in output of the second run and made CHEASE diverges when attempting a third run. The huge change of the current profile at the center influences a lot the safety factor profile. One then tried to impose the value of I^* at the center to remain constant by adding the boundary condition $I^*(0) = I_0^*(0)$. The resulting profiles are presented on figures 29. One can see that even though the first run seems to give better results, the second output I^* profile shows even bigger bumps than before.

Update only $\frac{d}{d\psi} \left(\frac{q}{C_2} \right)$

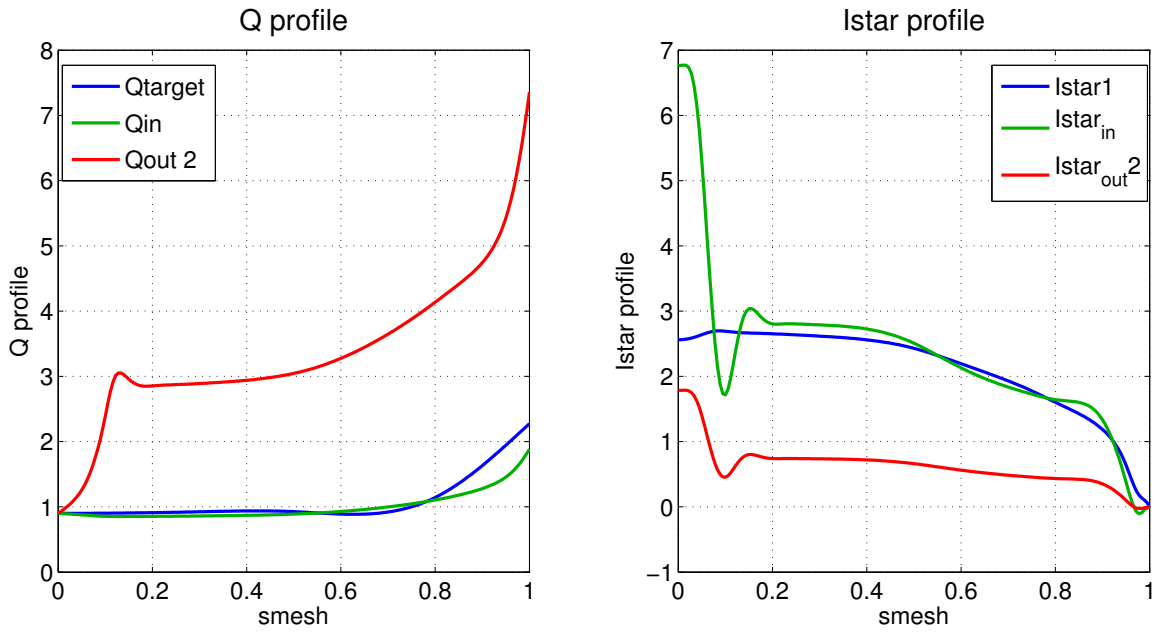
It appears in figure 30 that the I^* obtained from expression (15) with only the derivative term $\frac{d}{d\psi} \left(\frac{q}{C_2} \right)$ being updated is quasi-similar to the one with both terms updated. This shows that the derivative term is dominant in the expression of I^* and is thereby the one to be focused on. In figure 31 one can see that the derivative term actually initiates the bumps of I^* . Being multiplied by $4\pi^2$ in the second term of expression (15), the amplitude of the bumps grows bigger. Further investigations have shown that the C_1 surface integral (defined in equation (13)) has a weird shape from the first run which influences C_2 and of course $\frac{q}{C_2}$ and the I^* . This came from the $\frac{dV}{d\psi}$ term. By changing the I^* expression, one changes the current profile passing in each flux surface that is to say: one changes the $d\psi$. This explains the huge variation observed for $\frac{dV}{d\psi}$. In order to reduce this, one has tried to keep constant the quantity

$$\frac{dV}{d\psi} = \left(\frac{dV}{d\psi} \right)_0$$

In this case, the quantity $\frac{d}{d\psi} \left(\frac{q}{C_2} \right)$ only slightly changes but the bumps of the I^* are still steadily increasing over the runs which lead to a steadily diverging safety



(a) First run with only the q quantity updated



(b) Second run with only the q quantity updated

Figure 28: First two runs of CHEASE using expression (15) for input I^* with only the q quantity updated to q_{target} . Run have been made imposing boundary condition $I^*(edge) = 0$.

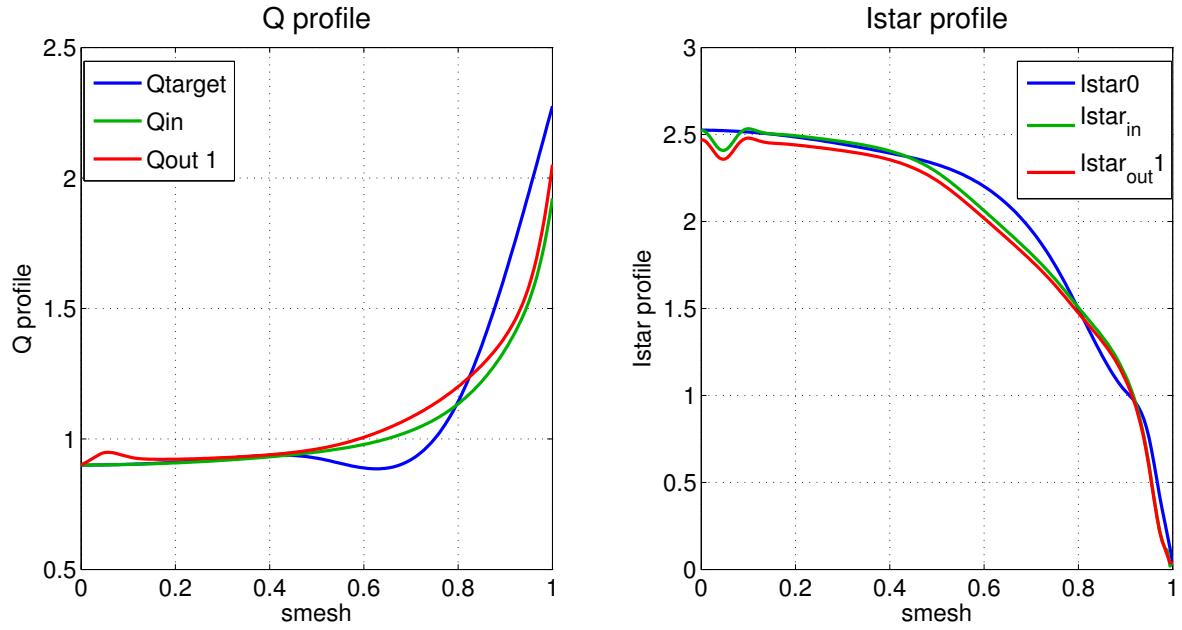
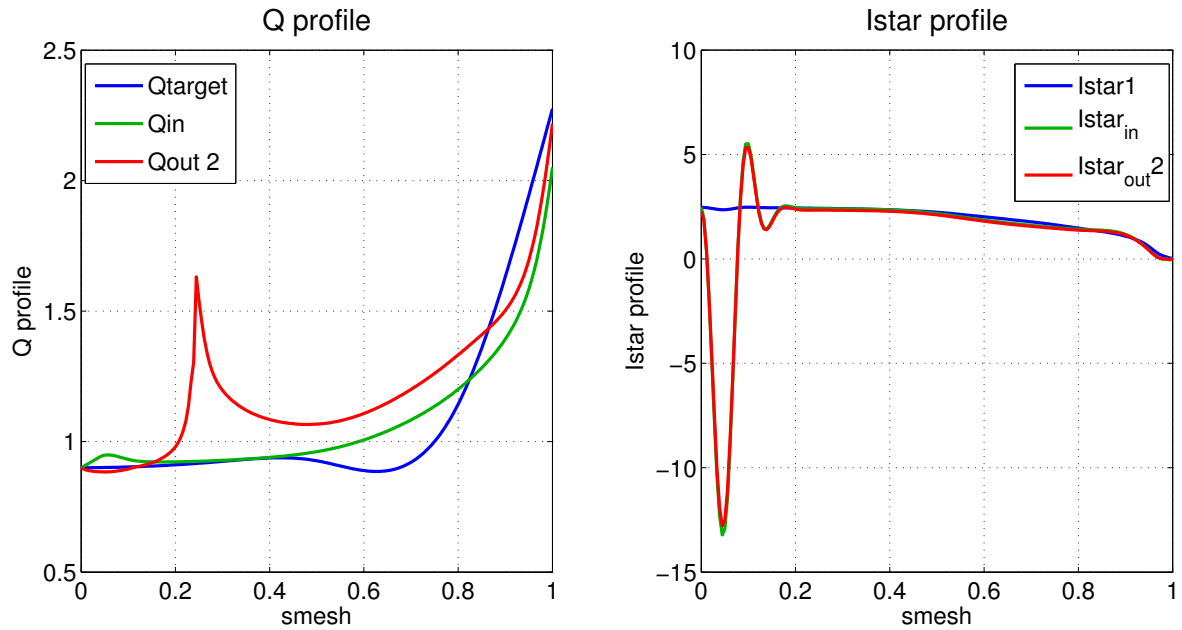
(a) First run with only the q quantity updated and $I^*(0) = I_0^*(0)$ (b) Second run with only the q quantity updated and $I^*(0) = I_0^*(0)$

Figure 29: First two runs of CHEASE using expression (15) for input I^* with only the q quantity updated to q_{target} . Runs have been made imposing boundary condition $I^*(edge) = 0$ and $I^*(0) = I_0^*(0)$.

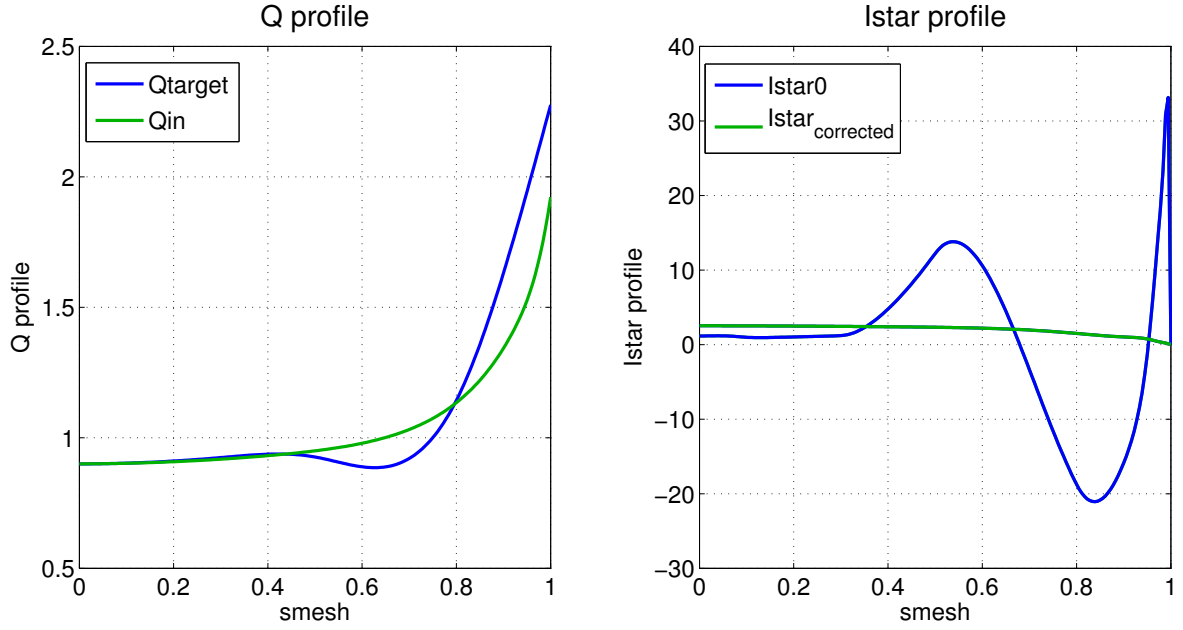


Figure 30: I^* profile obtained from equation (15) with only the derivative term $\frac{d}{d\psi} \left(\frac{q}{C_2} \right)$ updated.

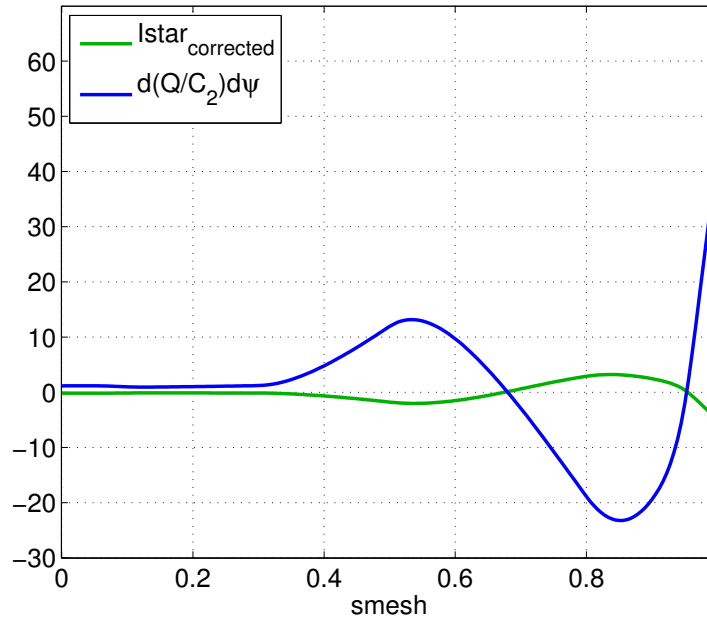


Figure 31: Slight oscillations of the derivative updated term $\frac{d}{d\psi} \left(\frac{q_{target}}{C_2} \right)$ induce the big bumps in I^* when multiplied by the other terms in the expression.

factor. One has to approach the problem differently. Another possibility was to derive with respect to a more stable quantity such as the volume V instead of the poloidal magnetic flux ψ , this leads us to the next appendix B.

B Deriving with respect to a more stable variable

Another approach was to derive $\frac{q}{C_2}$ with respect to the volume V rather than with respect to the poloidal magnetic flux ψ by re-expressing the surface averaged current density as:

$$I^* = \left(-\frac{C_1}{C_0} \right) * \left(p' + 8\pi^3 Q \frac{d}{dV} \left[\frac{Q}{C_2} \right] \right) \quad (65)$$

This change was motivated by the fact that the total volume V remains more con-

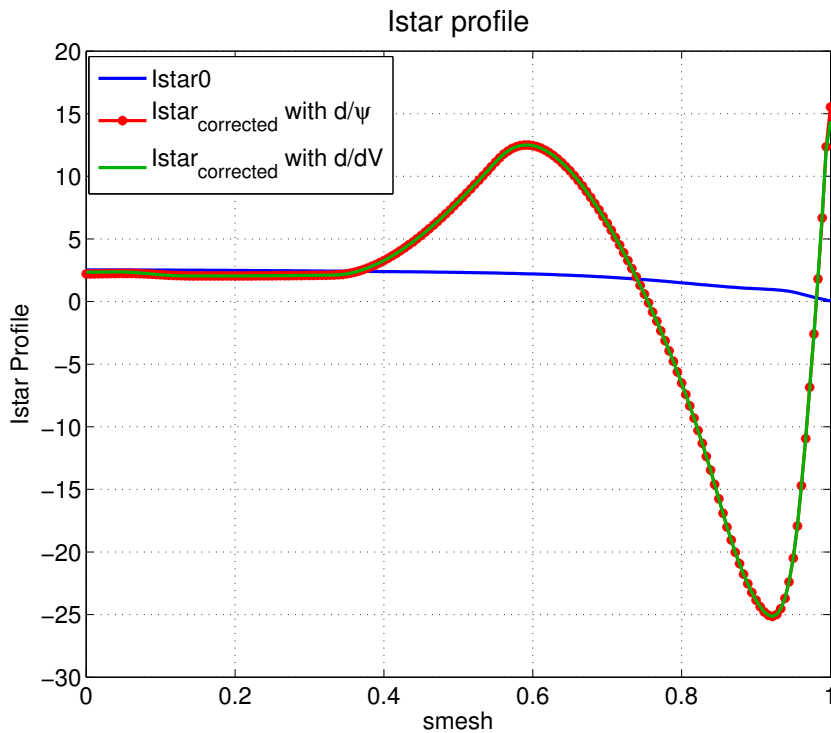
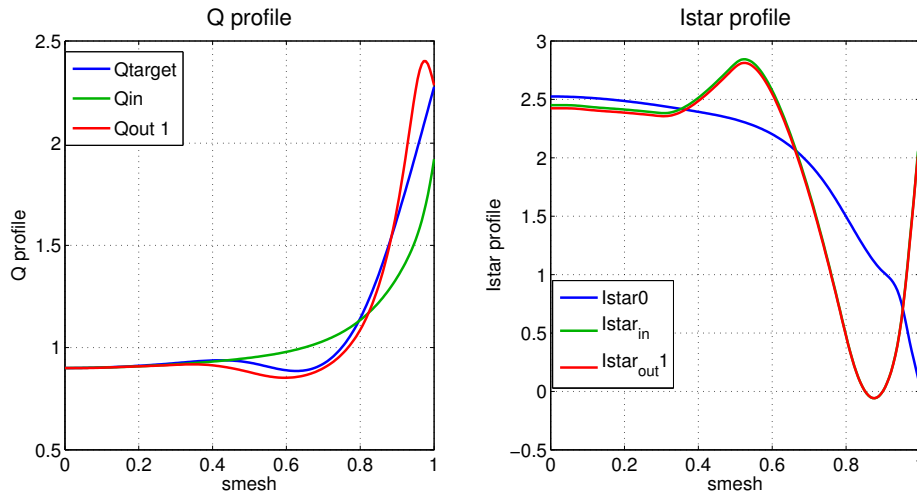
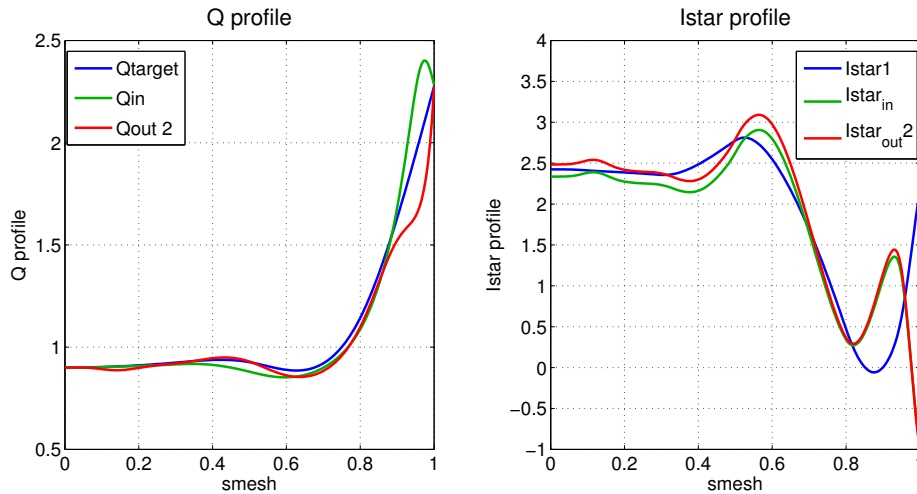


Figure 32: Plot of the expressions (15) and (65) (without the boundary condition to have a 0-value at the edge) respectively represented by the red and green curves. Their superimposition attests that the two formulas are equivalent.

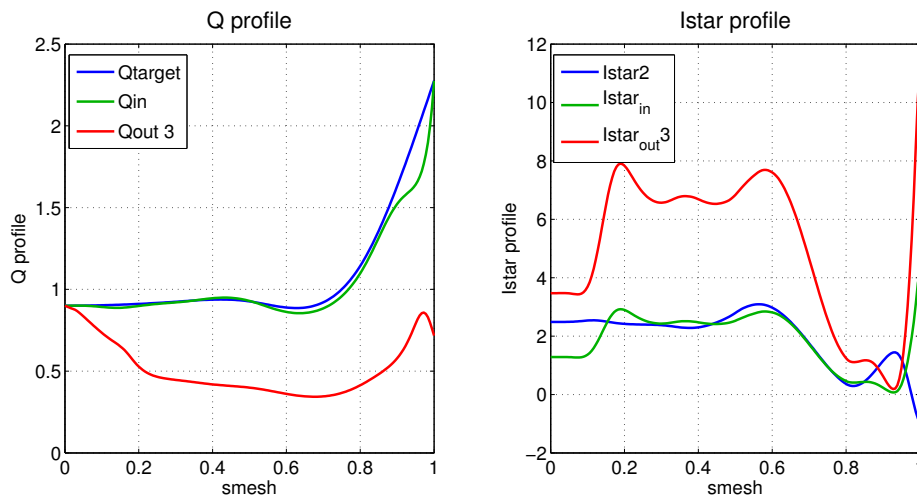
stant than ψ over the iterations to solve Grad-Shafranov equation. Indeed, as explained briefly above, while iterating to obtain convergence over the current density profile and over the surface coefficients, there is forward and backward substitution on ψ . Each time the current profile converges, the new flux surfaces are computed (with the new ψ solution) to see if the equilibrium coefficients converge too. Therefore, the poloidal magnetic flux profile ψ can be varying a lot from one iteration to the next one while the overall volume surrounding the flux surfaces remains nearly constant. Even if the shape of the exterior surface varies, the impact on the total inner volume will remain very small. The difference between figures 3 and figures 33 is that the second ones have been made with the derivative of $\frac{q}{C_2}$ calculated with respect to V instead of ψ and without the boundary condition imposing I^* to be 0 at the edge. With the same boundary condition, the two series of runs were exactly identical which indicates that it makes no improvement at all to derive with respect



(a) First run with $\alpha = 0.05$



(b) Second run with $\alpha = 0.05$



(c) Third run with $\alpha = 0.05$

Figure 33: Q and I^* profiles after a few runs of CHEASE using input I^* formula (65) (without the boundary condition to have a 0-value at the edge). Run done with $\alpha = 0.05$ and NFUNRHO=0.

to V than to ψ . Lots of boundary conditions and complementary fit have been tried here but unfortunately no improvement came without any side effect.

C Using $TT'(I^*)$ as input

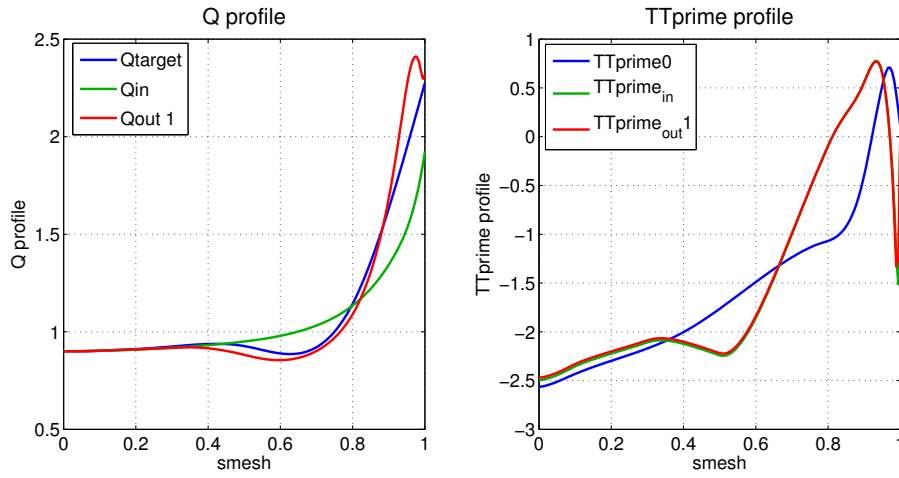
From equation (15), one can compute TT' as:

$$TT'_{target} = -\frac{C_0}{C_2} I_{target}^* - \frac{C_1}{C_2} p' \quad (66)$$

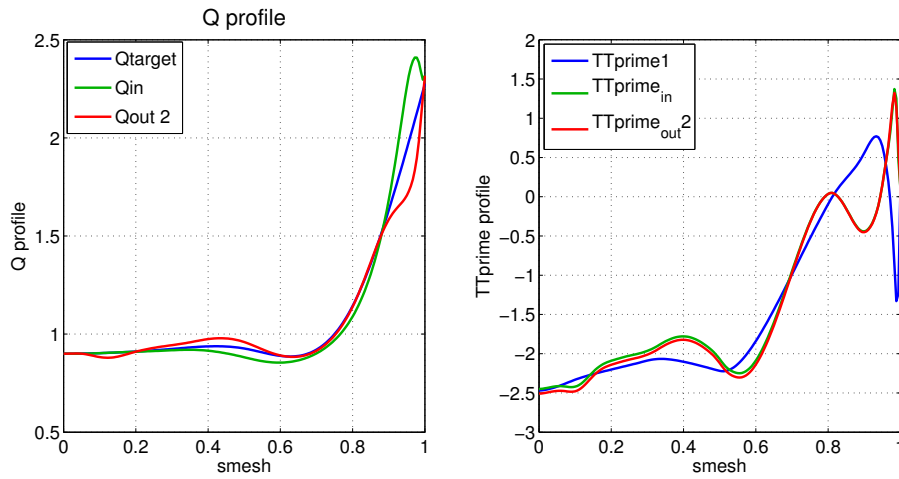
This consists of using the same I^* expression as before but to give it directly via TT' in input and therefore to try it with the case NSTTP = 1. Because of the oscillations of the I_{target}^* the α is still used:

$$TT'_{input,n} = \alpha \cdot TT'_{target} + (1 - \alpha) \cdot TT'_{n-1} \quad (67)$$

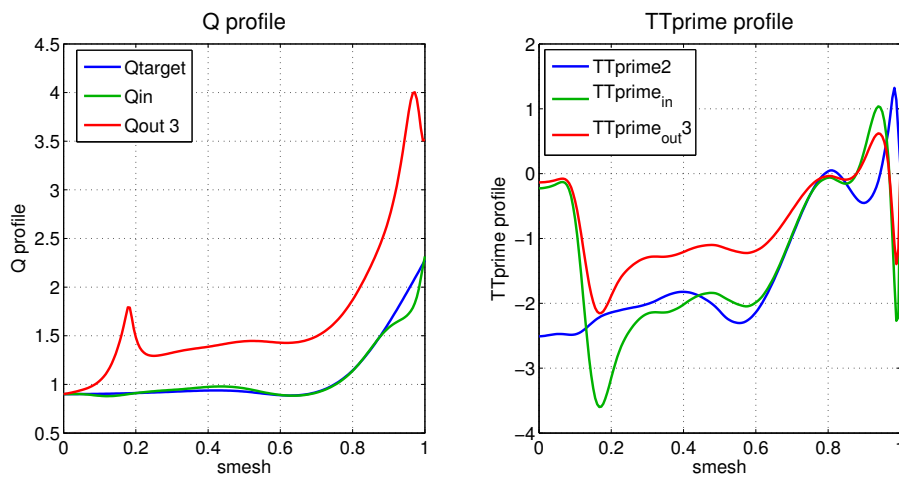
As before, $\alpha = 0.05$. The graphs 34 show that despite a first good output, very similar to the one obtained for NSTTP = 2 with the same bump at the edge, the output of the second run starts to oscillate which leads to steadily diverging profiles of q and TT' .



(a) q and TT' profiles after one external run of CHEASE using input TT' with $\alpha = 0.05$



(b) q and TT' profiles after two external runs of CHEASE using input TT' with $\alpha = 0.05$



(c) q and TT' profiles after three external runs of CHEASE using input TT' with $\alpha = 0.05$

Figure 34: Q and TT' profiles after a few runs of CHEASE using input $TT'(I^*)$. After a good start with the output of the first run, the TT' profile starts to oscillate which leads to a diverging safety factor profile. Run done with $\alpha = 0.05$ and $NFUNRHO = 0$. Run diverges immediately if tried with $NFUNRHO = 1$.

D Using an alternative radial coordinate: complement

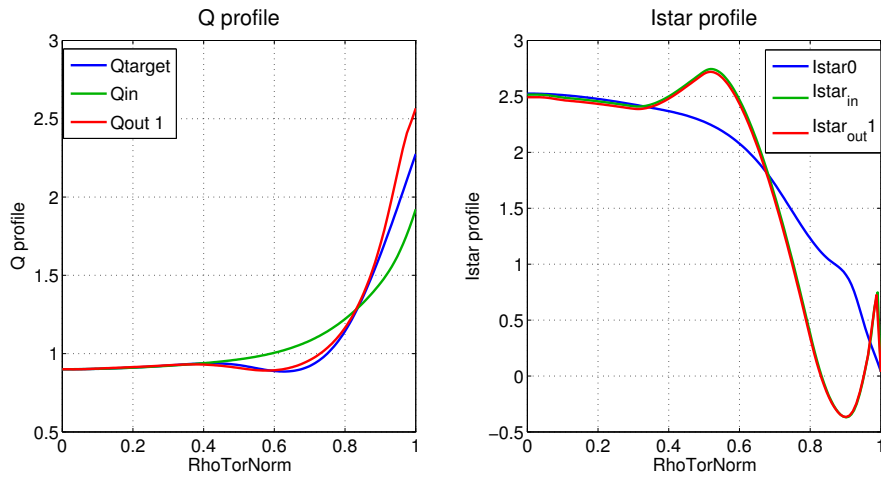
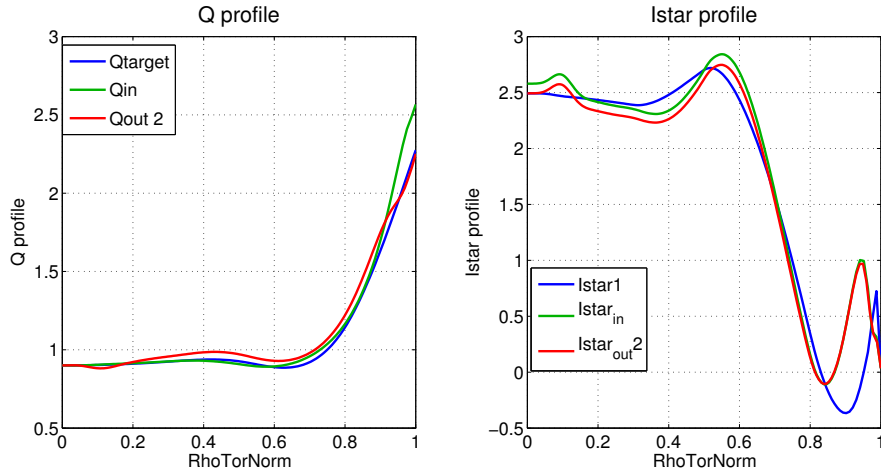
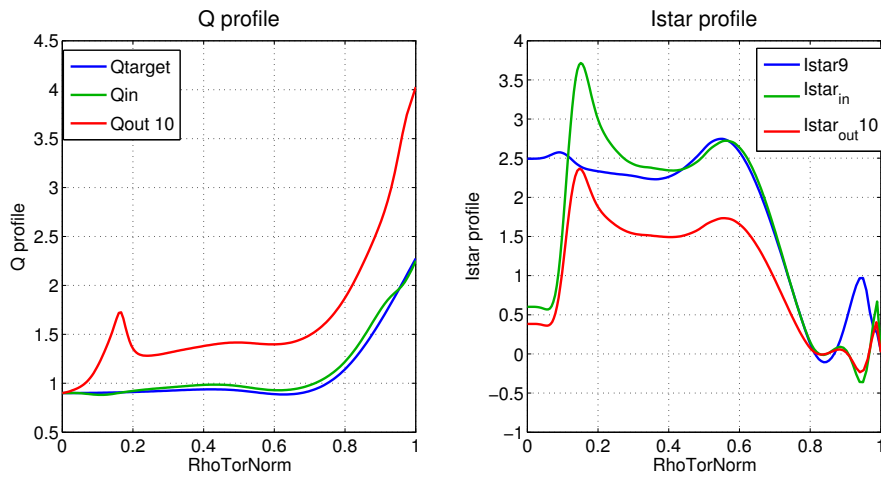
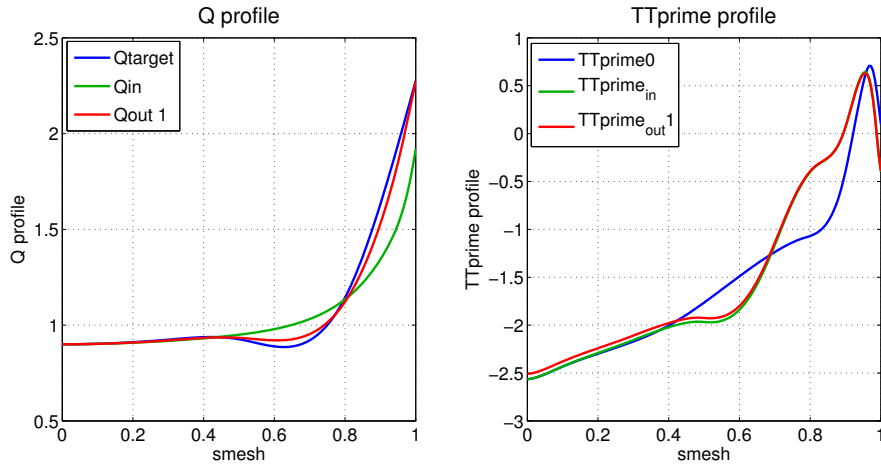
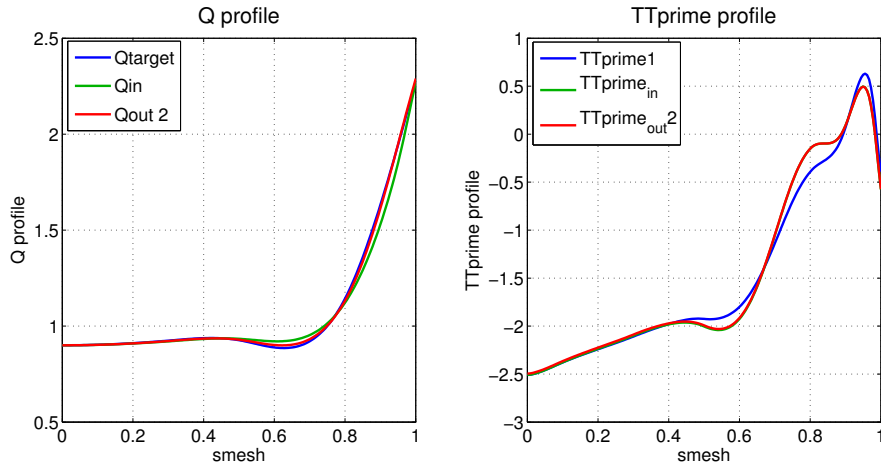
(a) First run with $\alpha = 0.05$ with $\rho_{toroidal}$ and $I^*(edge) = 0$ (b) Second run with $\alpha = 0.05$ with $\rho_{toroidal}$ and $I^*(edge) = 0$ (c) Third run with $\alpha = 0.05$ with $\rho_{toroidal}$ and $I^*(edge) = 0$

Figure 35: Q and I^* profiles after a few runs of CHEASE using input I^* formula (15). Even though the first run output is quite good, the next run shows the profiles to start oscillating and steadily diverging. Run done with $\alpha = 0.05$ and NFUNRHO=1.

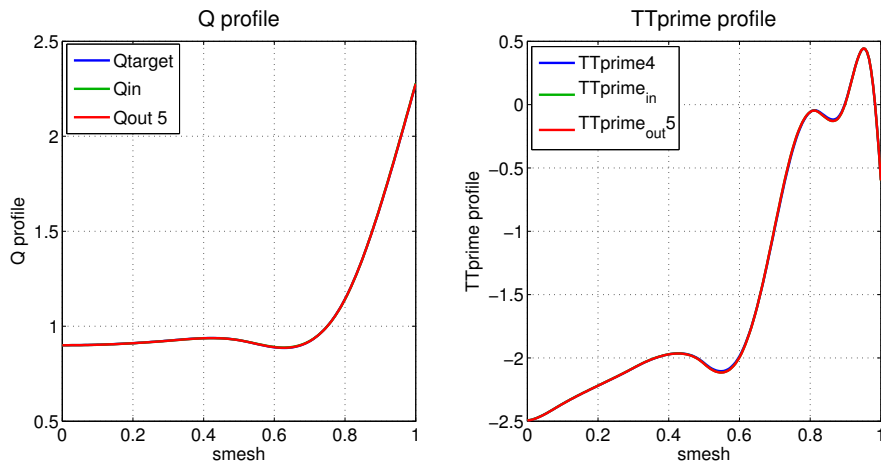
E I^* from Antoine Merle's note: complement



(a) q and TT' profiles after one external run of CHEASE using input $TT'(I^*)$



(b) q and TT' profiles after two external runs of CHEASE using input $TT'(I^*)$



(c) q and $TT'(I^*)$ profiles after five external runs of CHEASE using input TT'

Figure 36: Input TT' , NSTTP=1, NFUNRHO=0, $\alpha = 1$. Q and TT' profiles after a few runs of CHEASE using input TT' . The graphs show that the solution is steadily converging and leads to very good results.

References

- [1] *Sawteeth Module Development Notes*, A. MERLE, SPC, EPFL (2015).
- [2] *The CHEASE code for toroidal MHD equilibria*, H. LUTJENS, A. BONDESON, O. SAUTER, Computer Physics Communications (1995).
- [3] *Tokamak coordinate conventions: COCOS*, O. SAUTER, S.Yu. Medvedev, Computer Physics Communications (2012).
- [4] *MHD equilibrium and stability in Tokamacs*, J. P. Graves, SPC, EPFL (2011).
- [5] *Tearing mode in the cylindrical tokamak*, H. P. FURTH, P. H. RUTHERFORD and H. SELBERG, The Physics of Fluids (Volume 16, Number 7), Plasma Physics Laboratory, Princeton (1973).
- [6] *Normalizations on CHEASE*, O. SAUTER, SPC, EPFL (2013).
- [7] *Tokamaks* J. WESSON, third edition, Clarendon Press-Oxford (2004).
- [8] *Notes from the course of Plasma Physics III*, A. FASOLI, D. TESTA, A. HOWLING, I. FURNO, SPC, EPFL (2015).
- [9] *On magnetohydrodynamical equilibrium configurations*, V. D. SHAFRANOV, Soviet Physics JETP **6**, 545–554 (1958).
- [10] *Axisymmetrische magnetohydrodynamische Gleichgewichtskonfigurationen*, R. LUST & A. SCHLUTER, Z. Naturforsch. 12a, 850–854 (1957).
- [11] *Hydromagnetic equilibria and force-free fields*, H. GRAD & H. RUBIN, in Proc. 2nd Int. Conf. Peaceful Uses of Atomic Energy Vol. 31, 190–197 (United Nations, 1958).